NASA TECHNICAL NOTE

NASA TN D-3090

NASA TN D-3090

VIBRATION ANALYSIS OF CLUSTERED LAUNCH VEHICLES

by Rudolf F. Glaser and Everette E. Beam

George C. Marshall Space Flight Center
Huntsville, Ala.

NATIONAL AERONAUTICS AND SPACE ADMINISTRATION • WASHINGTON, D. C. • NOVEMBER 1965

NASA TN D-3090

VIBRATION ANALYSIS OF CLUSTERED LAUNCH VEHICLES

By Rudolf F. Glaser and Everette E. Beam

George C. Marshall Space Flight Center
Huntsville, Ala.

NATIONAL AERONAUTICS AND SPACE ADMINISTRATION

For sale by the Clearinghouse for Federal Scientific and Technical Information
Springfield, Virginia 22151 – Price $3.00

TABLE OF CONTENTS

LIST OF ILLUSTRATIONS

LIST OF ILLUSTRATIONS (Concluded)

LIST OF TABLES

DEFINITION OF SYMBOLS

Symbol	Definition
A	four x four matrix defined by the second equation 24
A_s	cross-sectional shear area
A_{si} $i = 1, 2..$	constant cross-sectional shear area between stations i and i + 1 of a lumped mass system (Fig. 6a)
B_1	four x four matrix defined by the first equation 32
B_i $i = 2, 3$	four x eight matrices defined by the second and third equations 32
$c = \frac{4e^2}{\delta}$	
$C_L = \begin{bmatrix} 0 & 0 & 0 & 0 \\ 0 & 0 & 0 & 0 \\ 0 & 0 & 0 & 0 \\ 0 & 0 & 0 & 0 \\ 0 & C_L & 0 & 0 \\ 0 & 0 & 0 & 0 \\ 0 & 0 & 0 & 0 \\ 0 & 0 & 0 & 0 \end{bmatrix}$	coefficient defined by equation 9
$C_M = \begin{bmatrix} 1 & 0 & 0 & 0 & 0 & 0 & 0 & 0 \\ 0 & 1 & 0 & 0 & 0 & 0 & 0 & 0 \\ 0 & 0 & c_{33} & 0 & c_{35} & 0 & 0 & 0 \\ 0 & 0 & 0 & 1 & 0 & 0 & 0 & 0 \\ 0 & 0 & c_{53} & 0 & c_{55} & 0 & c_{57} & 0 \\ 0 & 0 & 0 & 0 & 0 & 1 & 0 & 0 \\ 0 & 0 & 0 & 0 & c_{75} & 0 & c_{77} & 0 \\ 0 & 0 & 0 & 0 & 0 & 0 & 0 & 1 \end{bmatrix}$	coefficients defined by equation 10

DEFINITION OF SYMBOLS (Cont'd)

Symbol	Definition
C	eight x four matrix defined by the third equation 44
d_{ij} $i = 1, 2$; $j=1, 2, 3, 4$	eight-dimensional vector $d_{i1} = \begin{bmatrix} y_i^{(1)} \\ y_i^{(2)} \\ \cdot \\ \cdot \\ \cdot \\ y_i^{(8)} \end{bmatrix}$; $d_{i2} = f_i$; $d_{i3} = m_i$; $d_{i4} = q_i$
D_i $i = 1, 2, 3, 4$	eight x four matrices defined by the second equation 42
e	distance between outer lox tank axis and center beam vibration plane (Fig. 5)
E_i $i = 1, 2, 3, 4$	eight x eight matrices defined by the third equation 42
E	Young's modulus of elasticity
E_i	four x four matrix defined by equation A13
E_n	four x four matrix defined by equation A17
F	eight x four matrix defined by equations 35 and 47
$f_i = \begin{bmatrix} \Phi_i^{(1)} \\ \Phi_i^{(2)} \\ \cdot \\ \cdot \\ \cdot \\ \Phi_i^{(8)} \end{bmatrix} = d_{i2}$	
f, f_i $i = 1, 2 \ldots$	natural frequencies
G	eight x four matrix defined by the second equation 49
G	shear modulus of elasticity
H	eight x four matrix defined by the third equation 49

Symbol	Definition
I	eight x eight matrix defined by the third equation 47
I	cross-sectional moment of inertia of a beam
I_i $i = 1, 2, \ldots$	cross-sectional moment of inertia between stations i and i + 1 of a lumped mass system (Fig. 6a)
J	eight x four matrix defined by the first equation 49
$K = \begin{bmatrix} 0 & 0 & 0 & 0 & 0 & 0 & 0 & 0 \\ 0 & 0 & 0 & 0 & 0 & 0 & 0 & 0 \\ 0 & 0 & \kappa & 0 & 0 & 0 & 0 & 0 \\ 0 & 0 & 0 & 0 & 0 & 0 & 0 & 0 \\ 0 & 0 & 0 & 0 & 0 & 0 & 0 & 0 \\ 0 & 0 & 0 & 0 & 0 & 0 & 0 & 0 \\ 0 & 0 & 0 & 0 & 0 & 0 & \kappa & 0 \\ 0 & 0 & 0 & 0 & 0 & 0 & 0 & 0 \end{bmatrix}$	$\kappa = \frac{d_0^2}{2\delta_{SP}}$ spring stiffness of the outer lox tank support (spider section) Figure 5
k_1, k_n [lb/in]	spring stiffnesses of the supports 1, n of a lumped mass system (Fig. 6a)
$L_i = \begin{bmatrix} \ell_{11}^{(1)} & \ell_{12}^{(1)} & \ell_{13}^{(1)} & \ell_{14}^{(1)} \\ \ell_{21}^{(1)} & \ell_{22}^{(1)} & \ell_{23}^{(1)} & \ell_{24}^{(1)} \\ \ell_{31}^{(1)} & \ell_{32}^{(1)} & \ell_{33}^{(1)} & \ell_{34}^{(1)} \\ \ell_{41}^{(1)} & \ell_{42}^{(1)} & \ell_{43}^{(1)} & \ell_{44}^{(1)} \end{bmatrix}$ $i = 1, 2, 3$	transfer matrices of the center beam defined by Table 2
$L^{(F)} = \begin{bmatrix} \ell_{11}^{(F)} & \ell_{12}^{(F)} & \ell_{13}^{(F)} & \ell_{14}^{(F)} \\ \ell_{21}^{(F)} & \ell_{22}^{(F)} & \ell_{23}^{(F)} & \ell_{24}^{(F)} \\ \ell_{31}^{(F)} & \ell_{32}^{(F)} & \ell_{33}^{(F)} & \ell_{34}^{(F)} \\ \ell_{41}^{(F)} & \ell_{42}^{(F)} & \ell_{43}^{(F)} & \ell_{44}^{(F)} \end{bmatrix}$	transfer matrix of the outer fuel tank defined by Table 2

Symbol	Definition
$L^{(L)} = \begin{bmatrix} \ell_{11}^{(L)} & \ell_{12}^{(L)} & \ell_{13}^{(L)} & \ell_{14}^{(L)} \\ \ell_{21}^{(L)} & \ell_{22}^{(L)} & \ell_{23}^{(L)} & \ell_{24}^{(L)} \\ \ell_{31}^{(L)} & \ell_{32}^{(L)} & \ell_{33}^{(L)} & \ell_{34}^{(L)} \\ \ell_{41}^{(L)} & \ell_{42}^{(L)} & \ell_{43}^{(L)} & \ell_{44}^{(L)} \end{bmatrix}$	transfer matrix of the outer lox tank defined by Table 2
$L'_i \quad i = 1, 2$	four x four transfer matrix across branching point i (Table 3)
$L_2^* = L'_2 \; L_2 \; L'_1$	
$L = L_3 \; L_2^* \; L_1$	
$L_{ij} = \begin{bmatrix} \ell_{ij}^{(F)} & 0 & 0 & 0 & 0 & 0 & 0 & 0 \\ 0 & \ell_{ij}^{(L)} & 0 & 0 & 0 & 0 & 0 & 0 \\ 0 & 0 & \ell_{ij}^{(L)} & 0 & 0 & 0 & 0 & 0 \\ 0 & 0 & 0 & \ell_{ij}^{(F)} & 0 & 0 & 0 & 0 \\ 0 & 0 & 0 & 0 & \ell_{ij}^{(F)} & 0 & 0 & 0 \\ 0 & 0 & 0 & 0 & 0 & \ell_{ij}^{(L)} & 0 & 0 \\ 0 & 0 & 0 & 0 & 0 & 0 & \ell_{ij}^{(L)} & 0 \\ 0 & 0 & 0 & 0 & 0 & 0 & 0 & \ell_{ij}^{(F)} \end{bmatrix}$	$i, j = 1, 2, 3, 4$
L	transfer matrix defined by equations (All)
$\ell_i = x_{i+1} - x_i$	distance between stations i and i + 1 of a lumped mass system
$\Delta M_i' \quad i = 1, 2$	jump of the center beam bending moment at branching point i caused by the outer beam end moments
$\Delta M_i'' \quad i = 1, 2$	jump of the center beam bending moment at branching point i caused by the lox tank axial forces
$\Delta M_i = \Delta M_i' + \Delta M_i''$	$i = 1, 2$

DEFINITION OF SYMBOLS (Cont'd)

Symbol	Definition
M_i $i = 0, 1, 2, 3$	center beam bending moments at the top ($i = 0$) to the left of branching point 1 ($i = 1$), to the right of branching point 2 ($i = 2$), and at the vehicle end ($i = 3$)
M_i' $i = 1, 2$	center beam bending moments to the right of branching point 1 ($i = 1$) and to the left of branching point 2 ($i = 2$).
$M_i^{(j)}$ $i = 1, 2$; $j = 1, 2 \ldots 8$	end moments of the outer beam vibrations
$m_i = \begin{bmatrix} M_i^{(1)} \\ M_i^{(2)} \\ M_i^{(3)} \\ M_i^{(4)} \\ M_i^{(5)} \\ M_i^{(6)} \\ M_i^{(7)} \\ M_i^{(8)} \end{bmatrix}$	$i = 1, 2$
m_i $i = 1, 2 \ldots n$	lumped mass at station i of a lumped mass system
M	bending moment
M_i $i = 1, 2 \ldots n$	bending moment to the left of mass i of a lumped mass system
M_i^* $i = 1, 2 \ldots n$	bending moment to the right of mass i of a lumped mass system
N_{ij} $i, j = 1, 2$	eight x eight matrices defined by equations 46
$O = \begin{bmatrix} 0 \\ 0 \\ 0 \\ 0 \end{bmatrix}$	

DEFINITION OF SYMBOLS (Cont'd)

Symbol	Definition
P_i $i = 1, 2, \ldots n$	mass moment of inertia at station i of a lumped mass system
ΔQ_i $i = 1, 2$	jump of the center beam shearing force at branching point i caused by the outer beam support reactions
Q_i $i = 0, 1, 2, 3$	center beam shearing force at the top (i = 0), to the left of branching point 1 (i = 1), to the right of branching point 2 (i = 2), and at the vehicle end (i = 3)
Q_i' $i = 1, 2$	center beam shearing force to the right of branching point 1 (i = 1) and to the left of branching point 2 (i = 2)
$\pm Q_i^{(j)}$ $i = 1, 2$; $j = 1, 2..8$	support reactions of the outer beam vibrations
$q_i = \begin{bmatrix} Q_i^{(1)} \\ Q_i^{(2)} \\ Q_i^{(3)} \\ Q_i^{(4)} \\ Q_i^{(5)} \\ Q_i^{(6)} \\ Q_i^{(7)} \\ Q_i^{(8)} \end{bmatrix}$	$i = 1, 2$
Q	shearing force
Q_i	shear to the left of mass i of a lumped mass system
Q_i^*	shear to the right of mass i of a lumped mass system
$\mathbf{Q}$	eight x four matrix defined by equations 35

Symbol	Definition
R	four x four matrix defined by equation 31
R_i , i = 1, 2	eight x four matrices defined by equations 46
S_i i = 3, 5, 7	lox tank axial forces
$S_i = \begin{bmatrix} 1 & \ell_i & -\ell_i^2/2EI_i & -(\ell_i^3/6EI_i - \ell_i/GA_{si}) \\ 0 & 1 & -\ell_i/EI_i & -\ell_i^2/2EI_i \\ 0 & 0 & 1 & \ell_i \\ 0 & 0 & 0 & 1 \end{bmatrix}$ i = 1, 2... n-1	stiffness matrix of the i^{th} section of a lumped n- mass system
$T_i = \begin{bmatrix} 1 & 0 & 0 & 0 \\ 0 & 1 & 0 & 0 \\ 0 & \lambda P_i & 1 & 0 \\ -\lambda m_i & 0 & 0 & 1 \end{bmatrix}$	inertia matrix of the i^{th} mass of a lumped n- mass system
U	four x four unit matrix
$U_4^* = \begin{bmatrix} 0 & 0 & 0 & 0 \\ 0 & 0 & 0 & 0 \\ 0 & 1 & 0 & 0 \\ 0 & 0 & 0 & 0 \end{bmatrix}$	
$U_8^* = \begin{bmatrix} 0 & 0 & 0 & 0 & 0 & 0 & 0 & 0 \\ 0 & 0 & 0 & 0 & 0 & 0 & 0 & 0 \\ 0 & 0 & 1 & 0 & 0 & 0 & 0 & 0 \\ 0 & 0 & 0 & 0 & 0 & 0 & 0 & 0 \\ 0 & 0 & 0 & 0 & 1 & 0 & 0 & 0 \\ 0 & 0 & 0 & 0 & 0 & 0 & 0 & 0 \\ 0 & 0 & 0 & 0 & 0 & 0 & 1 & 0 \\ 0 & 0 & 0 & 0 & 0 & 0 & 0 & 0 \end{bmatrix}$	

DEFINITION OF SYMBOLS (Cont'd)

Symbol	Definition

$$V_3 = \begin{bmatrix} 0 & 0 & \dots & 0 & 0 \\ 0 & 0 & \dots & 0 & 0 \\ \cos \alpha_1 & 2 \cos \alpha_2 & \dots & 2 \cos \alpha_7 & \cos \alpha_8 \\ 0 & 0 & \dots & 0 & 0 \end{bmatrix}$$

$$V_4 = \begin{bmatrix} 0 & 0 & \dots & 0 & 0 \\ 0 & 0 & \dots & 0 & 0 \\ 0 & 0 & \dots & 0 & 0 \\ \cos \alpha_1 & 2 \cos \alpha_2 & \dots & 2 \cos \alpha_7 & \cos \alpha_8 \end{bmatrix}$$

$$V_1^* = \begin{bmatrix} \cos \alpha_1 & 0 & 0 & 0 \\ \cos \alpha_2 & 0 & 0 & 0 \\ \cos \alpha_3 & 0 & 0 & 0 \\ \cos \alpha_4 & 0 & 0 & 0 \\ \cos \alpha_5 & 0 & 0 & 0 \\ \cos \alpha_6 & 0 & 0 & 0 \\ \cos \alpha_7 & 0 & 0 & 0 \\ \cos \alpha_8 & 0 & 0 & 0 \end{bmatrix}$$

$$V_2^* = \begin{bmatrix} 0 & \cos \alpha_1 & 0 & 0 \\ 0 & \cos \alpha_2 & 0 & 0 \\ 0 & \cos \alpha_3 & 0 & 0 \\ 0 & \cos \alpha_4 & 0 & 0 \\ 0 & \cos \alpha_5 & 0 & 0 \\ 0 & \cos \alpha_6 & 0 & 0 \\ 0 & \cos \alpha_7 & 0 & 0 \\ 0 & \cos \alpha_8 & 0 & 0 \end{bmatrix}$$

x	abscissa
x_i	abscissa of station i of a lumped mass system
y_i $i = 0, 1, 2, 3, 4$	deflection of the vehicle top, $(i = 0)$, the branching points 1, 2 $(i = 1, 2)$, and the vehicle end $(i = 3)$
$y_i^{(j)}$ $i = 1, 2$; $j = ,1, 2, \dots 8$	deflections of the outer beam supports

DEFINITION OF SYMBOLS (Cont'd)

Symbol	Definition
y	deflection of a beam point
$y_i \quad i = 1, 2, \ldots n$	deflection of station i of a lumped mass system
$y_i = \begin{bmatrix} y_i \\ \Phi_i \\ M_i \\ Q_i \end{bmatrix} \quad i = 0, 1, 2, 3$	state vector at the vehicle top (i = 0), at the branching points 1, 2 (i = 1, 2), and at the vehicle end (i = 3)
$y_i^{(j)} = \begin{bmatrix} y_i \\ \Phi_i \\ M_i \\ Q_i \end{bmatrix} \quad i = 1, 2 \quad j = 1, 2 \ldots 8$	state vector of the j^{th} outer beam vibration at the supports 1, 2
$y_i = \begin{bmatrix} y_i \\ \varphi_i \\ M_i \\ Q_i \end{bmatrix} \quad i = 1, 2 \ldots n$	state vector to the left of station i of a lumped mass system
$y_i^* = \begin{bmatrix} y_i \\ \varphi_i \\ M_i^* \\ Q_i^* \end{bmatrix} \quad i = 1, 2 \ldots n$	state vector to the right of station i of a lumped mass system
$\alpha_i \quad i = 1, 2 \ldots 8$	angles between the y-axes of the center and outer beam vibration planes
$\delta_{SP} \left[\frac{in}{lb}\right]$	influence coefficient of the outer beam supports at the spider arms

DEFINITION OF SYMBOLS (Concluded)

Symbol	Definition
$\delta_o \left[\frac{in}{lb}\right]$	influence coefficient of the outer beam supports at the outriggers
$\delta_L \left[\frac{in}{lb}\right]$	lox tank influence coefficient
$\delta = \frac{\delta_{SP}}{2} + \delta_L + \frac{\delta_o}{2}$	
$\delta_1, \delta_n \left[\frac{in}{lb}\right]$	influence coefficients of the supports of a lumped mass system (Fig. 6a)
$\kappa = \frac{d_o^2}{2\delta_{SP}} \left[\frac{lb\ in}{rad}\right]$	spring stiffness of the outer lox tanks (spider section)
$\kappa_1, \kappa_n \left[\frac{lb\ in}{rad}\right]$	spring stiffness at the supports 1, n of a lumped mass system (Fig. 6a)
λ	parameter
$\lambda_i \quad i = 1, 2$	eigenvalues
$\sigma_1, \sigma_n \left[\frac{rad}{lb\ in}\right]$	influence coefficients at the supports of a lumped mass system (Fig. 6a)
$\Phi_i \quad i = 0, 1, 2, 3$	rotation angle at the vehicle top (i = 0), at the branching points 1, 2 (i = 1, 2), and at the vehicle end (i = 3)
$\Phi_i^{(j)} \quad i = 1, 2, ; \ j = 1, 2, .. 8$	end angles of the outer beams
φ	rotation angle of a beam point
$\varphi_i \quad i = 1, 2..n$	rotation angle at station i of a lumped mass system
ω	circular frequency

VIBRATION ANALYSIS OF CLUSTERED LAUNCH VEHICLES

SUMMARY

The Saturn I vehicle represents a complex ensemble of nine beams joined together. A first vibration analysis based on an equivalent single beam did not agree satisfactorily with the test results of the full scale test vehicle. Comparison of analysis and test results rather dictates that the coupling effects of the nine single beam vibrations can not be neglected. Hence, the analysis developed in this paper is based on a model consisting of nine clustered beams. However, the complexity of the system calls for many simplifying assumptions.

The basic idea of the analysis consists in coupling of the single beam vibrations such that the connections of the beams will be preserved. The method applied to the uncoupled single beams is the well known transfer matrix method. The mentioned coupling of the single beam vibrations leads to a linear homogeneous system of compatibility equations which must be solved during each transfer. Realization of the boundary conditions leads to a frequency curve indicating the coupled frequencies of the system. Finally the coupled mode shapes can be determined.

The analysis is programmed on IBM-709-4. Because it consists of simple matrix operations the computer time is short.

The results of an analysis of the Saturn I vehicle compare well with test results.

SECTION I. INTRODUCTION

The Saturn vehicle as shown by Figure 1 consists of payload, S-IV stage and S-I stage. In the S-I stage, eight clustered tanks (four fuel and four lox) are attached at each end to the center barrel (lox tank). Then, the Saturn vehicle represents a highly complex ensemble of nine beams joined together.

The results of a first vibration analysis based on an equivalent single beam did not agree satisfactorily with the test results of the full scale test vehicle (Ref. 1). The comparison of analysis and test results dictates that coupling can not be neglected; indeed, the vibrations of the nine single beams must be coupled.

Subsequently, several proposals concerning the vibration analysis of clustered booster vehicles have been made. Some of them are suggested by References 2, 3, and 4. The analysis shown herein is that done by the Dynamics and Loads Branch (Structures Division of the Propulsion and Vehicle Engineering Laboratory) George C. Marshall Space Flight Center.

This analysis is of a model outlined in Section III of this report. Complexity of the Saturn vehicle calls for many simplifying assumptions. But, remember the fundamental premise: the basic configuration of the model is a central beam with eight smaller beams clustered about it. From this premise, simplifications can be made concerning the mode of vibration, and the support conditions of the outer beams and single beam models. Assumptions about the mode of vibration are:

a. The center beam is restricted to plane vibrations in a symmetry plane of the vehicle through its long axis.

b. The outer beam vibrations occur symmetrically to this plane.

Nevertheless, each outer beam may have two planes of vibrations. The outer beam supports are assumed equivalent to either simple supports, or to simple supports having additional bending restraints. The single beams, finally, are modeled by lumped mass systems based on Timoshenko's beam theory.

The essential part of the analysis (Section IV) deals with the coupling of the single beam vibrations. The beams do not vibrate independently--they are connected. Coupling means adjustment of outer beam and center beam vibrations such that the connections of the beams will be preserved. In other words, certain conditions of compatibility must be satisfied. These circumstances can be expressed mathematically by a linear inhomogeneous system of equations to be solved.

The fundamental method applied in this analysis is the transfer matrix method. This method is well known (Ref. 5) but, for completeness a short explanation is given in the appendix. The transfer matrix method is based on the assumption that the beam masses and mass moments of inertia are lumped at stations of the beam axes. The state at each station is determined by a state vector which contains deflection, rotation angle, moment and shear at this station as components. The state vectors of successive stations are linked by transfer matrices. Such a transfer matrix is the product of an inertia and a stiffness matrix. In this way the transfer from one station to any other station of the beam is determined by a matrix which is composed of inertia and stiffness matrices. This applies especially to the end stations of the beam. These beam transfer matrices of the center and the outer beams are defined in Table 2. From the elements of these matrices the above mentioned compatibility equations can be formed and finally solved. Then the transfer of the complete system can be performed (Table 3). Now, realization of the boundary conditions leads to the eigenvalue equation. Evaluation of this equation and determination of the mode shapes form the final steps of the analysis.

The whole procedure outlined above will be done by application of simple matrix algebra. Formation, multiplication, inversion of low order matrices are the only operations performed. The matrices used and their dimensions are compiled in Table 4. The analysis is programmed on IBM-709-4. Because it consists of the mentioned simple matrix operations, the computer time is very short. To obtain one mode shape and frequency, approximately three minutes are necessary.

The results of an analysis of the Saturn I, SA-5 vehicle are presented and compare well with the test results. The mode shape characteristics of these complex shapes indicate the proper coupling model is used in the analysis.

SECTION II. MODEL

Before beginning discussion of the model used, a short description of the vehicle will be given (Fig. 1). The vehicle consists of payload, second stage and first stage. In the first stage, eight tanks are clustered symmetrically about a center tank. To connect outer tanks with the center tank, a spider beam at the upper end and the outrigger assembly on the lower end are used (Fig. 2). In addition, spider beam and outrigger assembly provide interconnection between stages and supports of the engines, respectively. The eight outer tanks consist of four lox tanks and four fuel tanks. The center tank is a lox tank.

The basic configuration of the model is, therefore, a center beam with eight smaller beams clustered symmetrically about it. Spider and outrigger structure provide supports of the outer beams.

The preparation of a vibration analysis of this system represents a difficult problem. The elastic, vibrating structure consists of a three-dimensional ensemble of non-uniform beams connected by the complex spider and outrigger structure. Obviously, the analysis must be based on a simplified model. On the other hand, analytic results based on too-simple models do not agree satisfactorily with the test results of the full scale test vehicle. Studies made, using different models, indicate that realistic assumptions concerning the outer beam supports are significant. Thus, to build up a mathematical model, two basic principles should be considered:

a. For analytic reasons a simplified model must be used.

b. To represent satisfactorily the dynamic behavior of the actual vehicle, the outer beam supports of the spider and tail sections must be modeled as closely as possible.

Some of the simplifying assumptions are usual and well known:

a. The nine beams of the vehicle model will be considered as Timoshenko beams.

b. The beam masses will be lumped at stations of the beam axes such that the stiffness between stations may be assumed as constant.

c. The liquid within the tanks will be assumed as solid--having mass, but no mass moment of inertia. The masses will be lumped like the other solid masses on the beam axes.

Another assumption deals with the vibration itself. Obviously a three-dimensional cluster, as in the Saturn vehicle, may vibrate in different modes depending on the nature of the excitation. For simplification, the analysis proposed is restricted to vibrations excited in a plane of symmetry. Cases (a) and (b) of Figure 3 show the positions of such planes within the cluster.[1] Then, the center beam vibration occurs in the symmetry plane. The outer beam vibrates symmetrically to this plane. Although the center beam vibration is in one plane, the outer beams must be expected to vibrate in two planes.

The analysis under discussion is based on case (a) of Figure 3. Yet, the analysis can be extended to case (b). On the other hand, test results of the full scale test vehicle do not indicate considerable deviations of mode shapes and frequencies of the cases (a), (b), and (c) shown by Figure 3.

The two planes of vibration of the outer beams can be assumed as radial and tangential planes (Fig. 4a). To distinguish among the different vibration planes, these planes will be numbered (Fig. 4a). For reasons of symmetry, restriction to one side of the vehicle is possible. The planes of radial vibrations are:

(1) (2) (4) (6) (8)

while tangential vibrations occur in the planes:

(3) (5) (7)

To measure deflections and rotation angles, coordinate systems must be assigned to each vibration plane (Fig. 4b). Hence the outer beam vibration planes may be characterized by the angles α_i = 1, 2, ... (8) between the y-axes of the center beam and outer beam vibration planes. Since only the cosine of these angles is important, the angles may be measured in arbitrary directions (Fig. 4a, Table 1).

---

1. It must be mentioned that these planes do not represent perfect symmetry planes since the arrangement of the outriggers is not symmetric to these planes (Figs. 4 and 5). However, the differences between both types of outriggers are so small--especially with regard to stiffness--that the outriggers can be considered as equal.

Now, the most important assumptions have to do with the outer beam supports located on spider arms and outriggers (Fig. 2). Spider arms and outriggers will be regarded as massless beams rigidly connected with the center beam at two branching points: Branching point 1 in the spider section, branching point 2 in the tail section. The flexibility of spider arms, and outriggers can be determined by the influence coefficients δ_{SP}, δ_0 respectively of the support points. The δ's are the deflections per unit load in direction of the tank axes. In view of the outer beam connections shown by Figure 2, the following assumptions can be made.

Spider section

In the radial planes of vibration (1), (2), (4), (6), (8), and in the tangential vibration plane (5) the outer beams behave like simple supported beams.

Hence, the boundary conditions are

$$\left.\begin{aligned} y_1^{(i)} &= y_1 \cos \alpha_i \\ M_1^{(i)} &= 0 \end{aligned}\right\} \qquad i = 1,\ 2,\ 4,\ 6,\ 8 \tag{1}$$

where $Y_1^{(i)}$, $M_1^{(i)}$ are deflection and moment of the i^{th} vibration at the spider supports and y_1 is the center beam deflection of branching point 1. Hence $y_1 \cos\alpha_i$ represents the support deflection in vibration plane (i) of the spider section caused by the center beam motion of branching point 1.

In the tangential planes of vibration (3) and (7) the outer beams behave like supported beams having additional bending restraints (spring constant χ).

This leads to the following boundary conditions:

$$\left.\begin{aligned} y_1^{(i)} &= y_1 \cos \alpha_i \ ;\ i = 3,\ 5,\ 7 \\ M_1^{(5)} &= 0 \\ M_1^{(i)} &= -\kappa\,(\varphi_1^{(i)} - \varphi_1 \cos \alpha_i) \ ;\ i = 3,\ 7 \end{aligned}\right\} \tag{2}$$

where $\varphi_1^{(i)}$, φ_1 are the rotation angles of the i^{th} outer beam and the center beam at branching point 1 respectively.

Figure 5 shows a schematic sketch of the support conditions of the tangential vibration planes. For convenience, the outer beam axes (in reality, situated on a cylinder around the center beam) are rolled up in the drawing plane. One concludes that the spring stiffness

$$\kappa = \frac{d_o^{\,2}}{2\,\delta_{SP}}$$

where d_o represents the outer tank diameter.

Since bending of the center beam causes rotation of the spider beam plane about the angle φ_1, the angles $\varphi_1^{(3)}$ and $\varphi_1^{(7)}$ are not the effective angles acting on the springs. Rather the effective angles are given by the parenthetical expression of the last two equations of the system 2.

Tail Section

In the radial planes of vibration (1), (2), (4), (6), (8), the outer beams can be considered again as simple supported beams. Hence, the boundary conditions of these planes may be written:

$$\left.\begin{aligned} y_2^{(i)} &= y_2 \cos \alpha_i \\ M_2^{(i)} &= 0 \end{aligned}\right\} \qquad i = 1,\ 2,\ 4,\ 6,\ 8 \tag{3}$$

where $y_2^{(i)}$, $M_2^{(i)}$ represent deflection and moment of the i^{th} outer beam vibration at the tail support and y_2 is the center beam deflection of branching point 2.

The beams vibrating in the tangential planes (3), (5), (7), may be regarded as supported beams having additional bending restraints. So, with regard to the deflections it follows

$$y_2^{(i)} = y_2 \cos \alpha_i \; ; \quad i = 3,\ 5,\ 7 \tag{4}$$

To obtain the remaining boundary conditions of the vibration planes (3), (5), (7), Figure 5 may be considered. It follows easily that

$$\left.\begin{aligned} \varphi_2^{(3)} - \varphi_2 \cos \alpha_3 &= (\eta_I - \eta_{II})/d_o \\ \varphi_2^{(5)} - \varphi_2 \cos \alpha_5 &= (\eta_{II} - \eta_{III})/d_o \\ \varphi_2^{(7)} - \varphi_2 \cos \alpha_7 &= (\eta_{III} - \eta_{IV})/d_o \end{aligned}\right\} \qquad (5)$$

where $\varphi_2^{(i)}$ is the rotation angle of the i^{th} outer beam vibration at the tail support and φ_2 represents the vibration angle of the center beam at branching point 1. η_i is the relative deflection of the support point i (i = I, II, III, IV). The terms on the left side of equations (5) represent the relative outer beam rotation angles at the support points which affect the existing springs.

Obviously, bending of the center beam can cause axial forces in the outer tanks. Still, from Figure 2, one realizes that axial forces may attack the outer lox tanks only. The outer fuel tanks may not resist axial forces because of their special supports in the spider section. Under consideration of the axial lox tank forces S_3 S_5 it follows from Figure 5 that

$$\left.\begin{aligned} \eta_I &= \left(\frac{M_2^{(3)}}{d_o} - \frac{S_3}{2}\right) \delta_o \\ \eta_{II} &= \left(\frac{M_2^{(5)} - M_2^{(3)}}{d_o} - \frac{S_3}{2}\right) \delta_o \\ \eta_{III} &= \left(\frac{M_2^{(7)} - M_2^{(5)}}{d_o} - \frac{S_7}{2}\right) \delta_o \\ \eta_{IV} &= \left(-\frac{M_2^{(7)}}{d_o} - \frac{S_7}{2}\right) \delta_o \end{aligned}\right\} \qquad (6)$$

Now, from Figure 5, it may be concluded

$$(\varphi_2 - \varphi_1)\ e = S_3 \left(\frac{\delta_{SP}}{2} + \delta_L + \frac{\delta_o}{2}\right)$$

where e is defined by Figure 5 and δ_L is the lox tank influence coefficient.

Setting

$$\frac{\delta_{SP}}{2} + \delta_L + \frac{\delta_o}{2} = \delta$$

one obtains

$$\left.\begin{aligned} S_3 &= \frac{e}{\delta}\ (\varphi_2 - \varphi_1) \\ \text{and similar} & \\ S_7 &= -\frac{e}{\delta}\ (\varphi_2 - \varphi_1) \end{aligned}\right\} \tag{7}$$

From (5), (6) and (7) it follows

$$\left.\begin{aligned} \varphi_2^{(3)} - \varphi_2 \cos\alpha_3 &= c_{33}\, M_2^{(3)} + c_{35}\, M_2^{(5)} \\ \varphi_2^{(5)} - \varphi_2 \cos\alpha_5 &= c_L\ (\varphi_2 - \varphi_1) + c_{53}\, M_2^{(3)} + c_{55}\, M_2^{(5)} + c_{57}\, M_2^{(7)} \\ \varphi_2^{(7)} - \varphi_2 \cos\alpha_7 &= c_{75}\, M_2^{(5)} + c_{77}\, M_2^{(7)} \end{aligned}\right\} \tag{8}$$

where

$$c_L = -\frac{e\delta_o}{d_o \delta} \tag{9}$$

$$\left.\begin{aligned} c_{33} = c_{53} = c_{77} &= \frac{2\delta_o}{d_o^{\,2}} \\ c_{35} = c_{53} &= -\frac{\delta_o}{d_o^{\,2}} \\ c_{37} = c_{75} &= -\frac{\delta_o}{d_o^{\,2}} \end{aligned}\right\} \tag{10}$$

Equations 3, 4, 8, 9, and 10 represent the complete boundary condition set of the outer tanks at the tail section.

At this point, some remarks will be made about coupling between the outer beam and the center beam vibrations. Obviously, these vibrations can not occur independently. The center beam distortions of branching point 1 and 2 influence the boundary conditions of the outer beams, while the outer beam support forces, and moments, contribute to shear and moment of the center beam at branching points 1 and 2.

Coupling exists also between the outer tank tangential vibrations. No direct coupling exists between the vibrations of radial planes (1), (2), (6), (8). Hence, the fuel tank modes of the planes (1), (8) and the lox tank modes of the planes (2) and (6) are equal to each other. (See Figs. 4 and 6)

In the above boundary conditions (1), (2), (3), (4), (8), the terms containing $\cos \alpha_i$ ($i = 1, 2, \ldots 3$) and c_L imply the coupling of the outer beam vibrations with the center beam vibration. The terms with the coefficient c_{ij}, $i, j = 3, 5, 7$ imply the coupling of the tangential plane vibrations (3), (5), (7), with each other.

Because

$$\cos \alpha_4 = \cos 90° = 0$$

the vibration of the radial plane (4) is uncoupled and so, does not contribute to the center beam vibration. Conversely, a vibration in plane (4) can not be excited since plane (4) is perpendicular to the assumed plane of excitation. For that reason, the radial vibration of plane (4) could have been omitted from this analysis without any loss of generality.

SECTION III. NUMERICAL RESULTS AND COMPARISON WITH TEST RESULTS

It is desirable to compare the results of the analysis with some dynamic test results in order to substantiate the analysis procedures and the mathematical model to the extent that sufficient structural detail was considered. The comparison can best be evaluated if the results of the analysis are considered first. The analysis, as described in this report, includes some interesting coupling of the outer tanks to the main beam. The dynamic test results which are available, also need some explanation since the test was a determination of transfer functions rather than a model survey.

Some typical mode shapes from the analysis are shown in Figures 7 to 16. (See also Fig. 6) Each figure represents a single mode of the total vehicle and can be identified, with some reservations, as either the center line of the vehicle bending in a first, second, or higher beam mode shape; or the bending of one of the outer tanks representing the major bending. The modes identified by vehicle center line are called "bending modes" and those identified by outer tanks are called "cluster modes." This identification can be rather useful in the evaluation of the analysis but can also offer some confusion in the proper presentation of results. The identification is maintained because of its usefulness in analysis and because of the similar identification of the dynamic test results.

The complication of a shape identification method can be seen if the mode shapes are studied as the fill level is lowered in the first stage of the vehicle to represent change of propellant with flight time. The simple and rather logical way to show the frequency trend throughout flight is to join the lowest frequency with a smooth curve, the next lowest, and so forth for the available data. As the total weight is reduced, the expectation would be for an increase in the frequency of the system. The frequency trend plotted in Figure 17 shows that this is true when these next lowest frequencies are connected. When sufficient fill conditions are used, the frequency trend lines will represent the frequency trends of the system.

Now the same data points can be joined by lines which represent the same mode shape trend from one time point to another. The trends of the "bending" modes and "cluster" modes are shown in Figure 18. The points on these curves between data points do not correspond to vehicle frequencies, with the exception of the line segments that happen to be identical to Figure 17. When this identification is used, the resulting curves can have a decrease in frequency as the fill level is lowered. This decrease does not show in Figure 18, but is not unusual. The curves also intersect and cross each other in a manner which can be described as the cluster modes crossing the center line bending modes. This crossing of the trends of Figure 18 brings up the question of crossing of the trends of Figure 17. These trends can cross, or come together, since cases can happen, and do happen where two modes of the system cannot be separated and a single frequency exists for two different mode shapes.

Now the test results will be considered. The dynamic testing is conducted by hanging the vehicle on a coil spring-cable suspension system in a special structural steel test tower. The cables are attached to the base of the booster stage and to the test tower at about the level of the top of the booster. A small angle is allowed between the cable from the vertical, and the springs between the cable and tower are as soft as practical. This system provides little lateral restraint and only a small end moment, which is necessary to maintain the vertical stability of the vehicle.

With the vehicle suspended in the tower, a single shaker is used to conduct the test program. The shaker is attached at the engine gimbal station of the first stage and transfer functions are determined for the one shaker location. The amplitude at the frequencies with maximum response is plotted and decay damping at these frequencies is determined. From these tests, the frequency trend curve and the "response mode shapes" will be used for comparison. The comparisons shown are as complete as practical and a few comments are in order.

The comparison of frequency trends is shown in Figure 19. The first bending mode frequencies compare favorably. The largest deviation is in the second mode and can be partly accounted for by the absence in the analysis of an engine mode representation. This has been added to later analysis and provides a better comparison. The test did not find an engine mode at all test points and is an example of the difficulty in obtaining all modes on the dynamic test vehicle.

The frequency comparison without mode shape comparison is not sufficient for such a system, therefore, the mode shapes are presented for the flight time of 35 seconds. The calculated mode shapes show good comparison to center line bending of the test modes. Some test mode shapes are compared with two calculated modes, since the test is a "response mode shape." The outer tanks do not compare as well in amplitude as the center line, since the tank response is generally lower. The comparison to more than one calculated mode shape and the difference in outer tank relative amplitude can partly be attributed to the type of test conducted.

The results from the analysis give good agreement with test results. It can be concluded that the structural connections and general structural parameters have been properly used since the mode shapes compare favorably with test results. The structural spring constants for tank coupling have been improved since this analysis and theoretical response analysis using the calculated mode shapes indicate the lower amplitude response of outer tanks is to be expected and the response of adjacent modes can be significant.

SECTION IV. ANALYSIS

The transfer matrix method as outlined in the appendix will now be applied to the developed model. The notations of the state vectors and transfer matrices are given in Tables 2 and 3. The simple transfers of the single beams (center beam, outer beams) may be seen from Table 2 while the transfer of the complete model is given by Table 3. The inertia and stiffness matrices T and S will be determined from the given vehicle data. (See appendix.) For this reason, the matrices L_1, L_2, L_3, $L_2^{(F)}$, $L_2^{(L)}$ which are composed of inertia and stiffness matrices (see appendix) can be considered as known.

From Table 3 of the transfer $0 \rightarrow 3$ of the model may be concluded as

$$\left.\begin{aligned} y_3 &= L_3 L_2' L_2 L_1' L_1 y_0 = L_3 L_2^* L_1 y_0 = L y_0 \\ L_2^* &= L_2' L_2 L_1' \\ L_S &= L_3 L_2^* L_1 \end{aligned}\right\} \qquad (11)$$

where

$$L_i = \begin{bmatrix} \ell_{11}^{(i)} & \ell_{12}^{(i)} & \ell_{13}^{(i)} & \ell_{14}^{(i)} \\ \ell_{21}^{(i)} & \ell_{22}^{(i)} & \ell_{23}^{(i)} & \ell_{24}^{(i)} \\ \ell_{31}^{(i)} & \ell_{32}^{(i)} & \ell_{33}^{(i)} & \ell_{34}^{(i)} \\ \ell_{41}^{(i)} & \ell_{42}^{(i)} & \ell_{43}^{(i)} & \ell_{44}^{(i)} \end{bmatrix} \qquad i = 1, 2, 3 \qquad (12)$$

L'_1 represents the transfer $1 \rightarrow 1'$ (over branching point 1) and L'_2 represents the transfer $2' \rightarrow 2$ (over branching point 2).

To perform the transfer $0 \rightarrow 3$ the matrices L'_1 and L_2^* must be known. The determination of these matrices represents the main problem of the analysis and will be done in two steps. First, L'_1 will be determined and then in a direct way L_2^*. L'_2 will not be determined explicitly.

The sketch on the top of Table 3 shows the vehicle model represented by the center beam axis. Because the outer beams are removed, external forces and moments must be applied to ensure equilibrium.

It follows, then, from this sketch:

$$y'_1 = y_1 + \begin{bmatrix} 0 \\ 0 \\ \Delta M_1 \\ \Delta Q_1 \end{bmatrix} . \qquad (13)$$

$$y_2 = y'_2 + \begin{bmatrix} 0 \\ 0 \\ \Delta M_2 \\ \Delta Q_2 \end{bmatrix} \qquad (14)$$

ΔQ_i, $i = 1, 2$ is the resultant of all outer beam support forces. One may, therefore, write:

$$\Delta Q_i = (-1)^i \left[Q_i^{(1)} \cos \alpha_1 + Q_i^{(8)} \cos \alpha_8 + 2 \sum_{j=2}^{7} Q_i^{(j)} \cos \alpha_j \right] ; \; i = 1, 2$$

where

$Q_i^{(j)}$; $i = 1, 2$; $j = 1, 2 \ldots 8$ are the shears at the outer beam supports.

Using vector and matrix notation, one may write:

$$\begin{bmatrix} 0 \\ 0 \\ 0 \\ \Delta Q_j \end{bmatrix} = (-1)^i \, V_4 \, q_i ; \; i = 1, 2 \qquad (15)$$

where

$$V_4 = \begin{bmatrix} 0 & 0 & 0 & 0 \\ 0 & 0 & 0 & 0 \\ 0 & 0 & 0 & 0 \\ \cos \alpha_1 & 2 \cos \alpha_2 \ldots & 2 \cos \alpha_7 & \cos \alpha_8 \end{bmatrix} \tag{16}$$

and

$$q_i = \begin{bmatrix} Q_i^{(1)} \\ Q_i^{(2)} \\ . \\ . \\ . \\ Q_i^{(8)} \end{bmatrix} \quad ; \; i = 1, 2 \tag{17}$$

ΔM_i is caused not only by the outer beam support reactions, there is also a contribution of the lox tank axial forces. ΔM_i can, therefore, be written:

$$\Delta M_i = \Delta M_i' + \Delta M_i'' \quad ; \quad i = 1, 2 \tag{18}$$

where

$\Delta M_i''$ represents the moment contribution of the outer lox tank axial forces.

$\Delta M_i'$ can be expressed similar to equation 15

$$\begin{bmatrix} 0 \\ 0 \\ \Delta M_i' \\ 0 \end{bmatrix} = (-1)^i \; V_3 \; m_i \qquad i = 1, 2 \tag{19}$$

where

$$m_i = \begin{bmatrix} M_i^{(1)} \\ M_i^{(2)} \\ . \\ . \\ . \\ M_i^{(8)} \end{bmatrix} \qquad i = 1, 2 \tag{20}$$

and V_3 results from the matrix 16 by changing third and fourth row.

The second term of 18 may be obtained from Figure 5 and equation 7 as

$$\Delta M_i'' = 2(-1)^{i+1}\, 2eS_3 = (-1)^{i+1}\,\frac{4e^2}{\delta}\,(\varphi_2 - \varphi_1)$$

or

$$\begin{bmatrix} 0 \\ 0 \\ \Delta M_i'' \\ 0 \end{bmatrix} = (-1)^{i+1}\, c\; U^*_4\,(y_2' - y_1') \qquad i = 1, 2 \tag{21}$$

where

$$c = \frac{4e^2}{\delta}$$

and

$$U^*_4 = \begin{bmatrix} 0 & 0 & 0 & 0 \\ 0 & 0 & 0 & 0 \\ 0 & 1 & 0 & 0 \\ 0 & 0 & 0 & 0 \end{bmatrix} \tag{22}$$

In equation 21 y_2' may be replaced by

$$y_2' = L_2\, y_1' \tag{23}$$

(Table 3) then it follows

$$\left.\begin{bmatrix} 0 \\ 0 \\ \Delta M_i'' \\ 0 \end{bmatrix} = (-1)^{i+1}\; c\; A\; y_1' \qquad i = 1, 2 \right\} \tag{24}$$

$$A = U_4^*\,(L_2 - U_4)$$

where U_4 is the four x four unit matrix.

From equations 13, 15, 19, 24 it follows:

$$y_1' = y_1 - V_4\, q_1 - V_3\, m_1 + c\, A\, y_1' \tag{25}$$

Now to replace m, the boundary conditions (1) and (2) with regard to $M_1^{(j)}$ j = 1, 2. . . . . 8, may be introduced. These conditions, written in vector notation are:

$$m_1 = - K f_1 + K V_2^* y_1 \tag{26}$$

where

$$K = \begin{bmatrix} 0 & 0 & 0 & 0 & 0 & 0 & 0 & 0 \\ 0 & 0 & 0 & 0 & 0 & 0 & 0 & 0 \\ 0 & 0 & \kappa & 0 & 0 & 0 & 0 & 0 \\ 0 & 0 & 0 & 0 & 0 & 0 & 0 & 0 \\ 0 & 0 & 0 & 0 & 0 & 0 & 0 & 0 \\ 0 & 0 & 0 & 0 & 0 & 0 & 0 & 0 \\ 0 & 0 & 0 & 0 & 0 & 0 & \kappa & 0 \\ 0 & 0 & 0 & 0 & 0 & 0 & 0 & 0 \end{bmatrix} \tag{27}$$

$$f_i = \begin{bmatrix} \varphi_i^{(1)} \\ \varphi_i^{(2)} \\ . \\ . \\ . \\ \varphi_i^8 \end{bmatrix} \qquad i = 1, 2 \tag{28}$$

$$V^*_2 = \begin{bmatrix} 0 & \cos \alpha_1 & 0 & 0 \\ 0 & \cos \alpha_2 & 0 & 0 \\ 0 & \cos \alpha_3 & 0 & 0 \\ 0 & \cos \alpha_4 & 0 & 0 \\ 0 & \cos \alpha_5 & 0 & 0 \\ 0 & \cos \alpha_6 & 0 & 0 \\ 0 & \cos \alpha_7 & 0 & 0 \\ 0 & \cos \alpha_8 & 0 & 0 \end{bmatrix} \tag{29}$$

Insertion of equation 26 into equation 25--and little algebra--yields

$$(U_4 - c A) y_1' = (U_4 - V_3 K V_2^*) y_1 + V_3 K f_1 - V_4 q_1 \tag{30}$$

Setting

$$(U_4 - c A)^{-1} = U_4 + \frac{c}{1 - c l_{23}^{(2)}} A = R \tag{31}$$

and

$$\left.\begin{aligned} R\,(U_4 - V_3\,K\,V_2^{*}) &= B_1 \\ R\,V_3\,K_1 &= -B_2 \\ R\,V_4 &= B_3 \end{aligned}\right\} \tag{32}$$

equation 30 changes over in

$$y_1' = B_1\,y_1 - B_2\,f_1 - B_3\,q_1 \tag{33}$$

The relation 31 may be proved easily by verifying

$$(U - c\,A)\,(U + \frac{c}{1 - c\,l_{23}^{(2)}}\,A) = U$$

From equations 14, 15, 19, 23, 24 one obtains

$$y_2 = (L_2 - c\,A)\,y_1' + V_3\,m_2 + V_4\,q_2 \tag{34}$$

Equation 34 will be needed later on.

In equation 33 the sixteen components of the vectors f_1 and q_1 represent the unknowns of the problem in hand. In the following it will be shown that f_1 and q_1 can be determined by the outer beam boundary conditions of the tail section. From these conditions it will be concluded:

$$\left.\begin{aligned} f_1 &= F\,y_1 \\ q_1 &= Q\,y_1 \end{aligned}\right\} \tag{35}$$

where F and Q are eight x four matrices.

Then, combining equations 33 and 35, one obtains

$$y_1' = (B_1 - B_2\,F - B_3\,Q)\,y_1 \tag{36}$$

and hence (see Table 3)

$$L_1' = B_1 - B_2\,F - B_3\,Q \tag{37}$$

To determine the matrices F and Q of equations 35 the transfers of the outer beams must be considered. In doing so, it is convenient to use the following notations:

$$d_{i1} = \begin{bmatrix} y_i^{(1)} \\ y_i^{(2)} \\ . \\ . \\ . \\ y_i^{(8)} \end{bmatrix} ; \quad d_{i2} = f_i ; \; d_{i3} = m_i ; \; d_{i4} = q_i \qquad (38)$$

$$i = 1, 2$$

where q_i, m_i, f_i are defined by equations 17, 20, and 28, respectively.

Then the outer beam transfers (Table 2) may be written:

$$d_{2k} = \sum_{j=1}^{4} L_{kj} d_{1j}; \quad k = 1, 2, 3, 4 \qquad (39)$$

where

$$L_{kj} = \begin{bmatrix} \ell_{kj}^{(F)} & 0 & 0 & 0 & 0 & 0 & 0 & 0 \\ 0 & \ell_{kj}^{(L)} & 0 & 0 & 0 & 0 & 0 & 0 \\ 0 & 0 & \ell_{kj}^{(L)} & 0 & 0 & 0 & 0 & 0 \\ 0 & 0 & 0 & \ell_{kj}^{(F)} & 0 & 0 & 0 & 0 \\ 0 & 0 & 0 & 0 & \ell_{kj}^{(F)} & 0 & 0 & 0 \\ 0 & 0 & 0 & 0 & 0 & \ell_{kj}^{(L)} & 0 & 0 \\ 0 & 0 & 0 & 0 & 0 & 0 & \ell_{kj}^{(L)} & 0 \\ 0 & 0 & 0 & 0 & 0 & 0 & 0 & \ell_{kj}^{(F)} \end{bmatrix} \qquad (40)$$

$$k,j = 1, 2, 3, 4$$

Application of the notation 38 to the boundary conditions: equations 1, 2, and 26, respectively, yields

$$\left.\begin{aligned} d_{11} &= V_1^* y_1 \\ d_{13} &= m_1 = -K f_1 + K V_2^* y_1 \end{aligned}\right\} \qquad (41)$$

where K and V_2^* are given by equations 27 and 29. V_1^* follows from the matrix 29 by changing the first two columns.

Equations 39, 40, 41 result in

$$\left.\begin{aligned} d_{2i} &= D_i y_1 + E_i f_1 + L_{i4} q_1 \\ \text{where} \\ D_i &= L_{i1} V_1^* + L_{i3} K V_2^* \\ E_i &= L_{i2} - L_{i3} K \end{aligned}\right\} \qquad (42)$$

$$i = 1, 2, 3, 4$$

As already mentioned, the boundary conditions 3, 4, 8, will now serve for determination of f_1 and q_1. Using the vector notation 38 these conditions may be written:

$$\left.\begin{aligned} d_{21} &= V_1^* y_2' \\ U_8^* (d_{22} - V_2^* y_2') &= C_L (y_2' - y_1') + C_M d_{23} \end{aligned}\right\} \qquad (43)$$

where

$$U_8^* = \begin{bmatrix} 0&0&0&0&0&0&0&0 \\ 0&0&0&0&0&0&0&0 \\ 0&0&1&0&0&0&0&0 \\ 0&0&0&0&0&0&0&0 \\ 0&0&0&0&1&0&0&0 \\ 0&0&0&0&0&0&0&0 \\ 0&0&0&0&0&0&1&0 \\ 0&0&0&0&0&0&0&0 \end{bmatrix} \quad ; \quad C_L = \begin{bmatrix} 0&0&0&0 \\ 0&0&0&0 \\ 0&0&0&0 \\ 0&0&0&0 \\ 0&C_L&0&0 \\ 0&0&0&0 \\ 0&0&0&0 \\ 0&0&0&0 \end{bmatrix}$$

$$C_M = \begin{bmatrix} 1 & 0 & 0 & 0 & 0 & 0 & 0 & 0 \\ 0 & 1 & 0 & 0 & 0 & 0 & 0 & 0 \\ 0 & 0 & C_{33} & 0 & C_{35} & 0 & 0 & 0 \\ 0 & 0 & 0 & 1 & 0 & 0 & 0 & 0 \\ 0 & 0 & C_{53} & 0 & C_{55} & 0 & C_{57} & 0 \\ 0 & 0 & 0 & 0 & 0 & 1 & 0 & 0 \\ 0 & 0 & 0 & 0 & C_{75} & 0 & C_{77} & 0 \\ 0 & 0 & 0 & 0 & 0 & 0 & 0 & 1 \end{bmatrix}$$

The elements C_L; C_{ij}; i, j = 3, 5, 7 are given by equations 9 and 10.

Insertion of equation 23 into equation 43 and collection of terms yields

$$\left.\begin{aligned} d_{21} &= V_1^* L_2 y_1' \\ U_8^* d_{22} - C_M d_{23} &= C y_1 \end{aligned}\right\} \qquad (44)$$

where

$$C = (U_8^* V_2^* + C_L) L_2 - C_L$$

Now, replacement of y_1', d_{21}, d_{22}, d_{23} by equations 33 and 42 changes the first two equations 44 over in

$$\left.\begin{aligned} N_{11} q_1 + N_{12} f_1 &= R_1 y_1 \\ N_{21} q_1 + N_{22} f_2 &= R_2 y_2 \end{aligned}\right\} \qquad (45)$$

where

$$\left.\begin{aligned} N_{11} &= L_{14} + V_1^* L_2 B_3 \\ N_{12} &= E_1 + V_1^* L_2 B_2 \\ R_1 &= -D_1 + V_1^* L_2 B_1 \\ N_{21} &= U_8^* L_{24} + C B_3 - C_M L_{34} \\ N_{22} &= U_8^* E_2 + C B_2 - C_M E_3 \\ R_2 &= -U_8^* D_2 + C B_1 + C_M D_3 \end{aligned}\right\} \qquad (46)$$

The matrices N_{ij} $i,j = 1, 2$ are eight x eight matrices, while R_1 R_2 are eight x four matrices. Solution of this system is given by equations 35 where

$$\left.\begin{aligned} F &= I^{-1}\,[R_1 - N_{11}\,N_{21}^{-1} R_2] \\ Q &= N_{21}^{-1}\,[-N_{22}\,I^{-1} R_1 + N_{22}\,I^{-1} N_{11}\,N_{21}^{-1} R_2 + R_2] \\ I &= N_{12} - N_{11}\,N_{21}^{-1} N_{22} \end{aligned}\right\} \qquad (47)$$

Proof by insertion.

Obviously the system of equation 45 is solvable only if the matrices I and N_{21} are nonsingular matrices.

Now from equations 37 and 47 it follows that L_1' is known.

To determine L_2^* given by the second equation 11 and Table 3, one may start from equation 34. Considering equations 33, 35, and 42 it follows from equation 34:

$$y_2 = (J + g\,F + H\,Q)\,y_1 = L_2^*\,y_1 \qquad (48)$$

where
$$\left.\begin{aligned} J &= V_3\,D_3 + V_4\,D_4 + (L_2 - c\,A)\,B_1 \\ g &= V_3\,E_3 + V_4\,E_4 - (L_2 - c\,A)\,B_2 \\ H &= V_3\,L_{34} + V_4\,L_{44} - (L_2 - c\,A)\,B_3 \end{aligned}\right\} \qquad (49)$$

Because of 47, 48, and 49 L_2^* is known and hence

$$L = L_3\,L_2^*\,L_1$$

also (See eq. 13). In this way, the frequency equation of the system can be solved as outlined in the appendix. The solutions are the eigenvalues

$$\lambda_1 = \omega_1^2 \;;\; \lambda_2 = \omega_2^2 \ldots$$

Now the start vectors y_o can be determined.

y_o is the start vector of the center beam part between top 0 and branching point 1. The start vector of the center beam between branching points 1 and 2 is given by

$$L_1'\,L_1\,y_0$$

The start vectors, vectors of the outer beam vibrations, are

$$\begin{bmatrix} y_1^{(i)} \\ \varphi_1^{(i)} \\ M_1^{(i)} \\ Q_1^{(i)} \end{bmatrix} \qquad i = 1, 2, \ldots 8$$

The components of these start vectors follow from equations 35, 41, and 47, where

$$y_1 = L_1 y_0$$

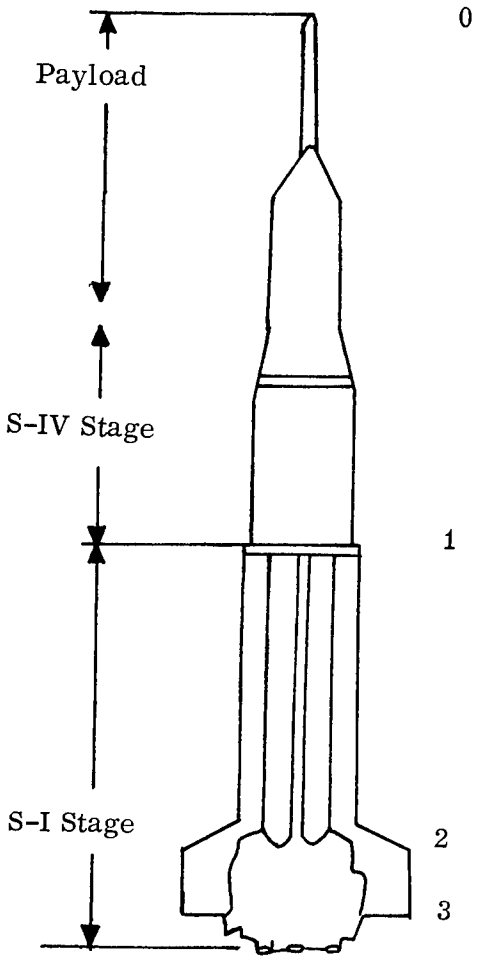

FIGURE 1. SATURN SA-7

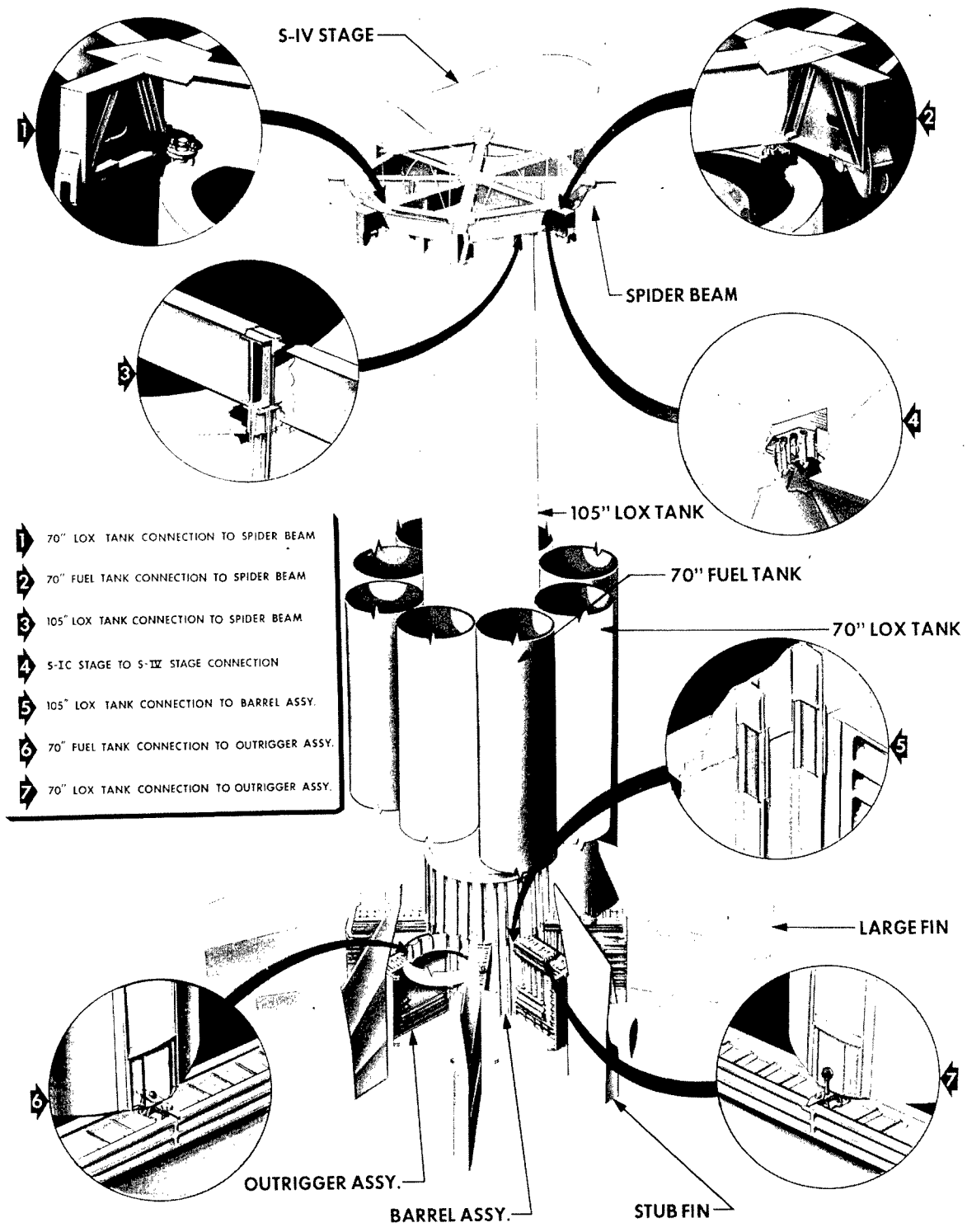

FIGURE 2. SATURN I BLOCK II CONNECTION DETAILS

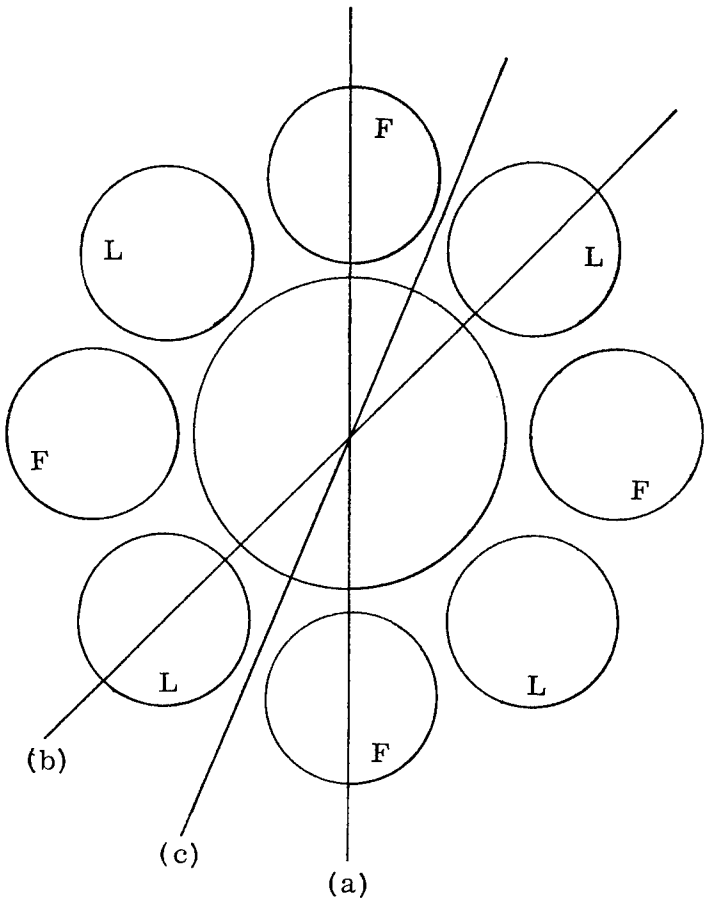

F --- Fuel Tank
L --- Lox Tank

FIGURE 3. PLANES OF EXCITATION

T. . . . Thrust Outrigger
F. . . . Fin Outrigger

a)

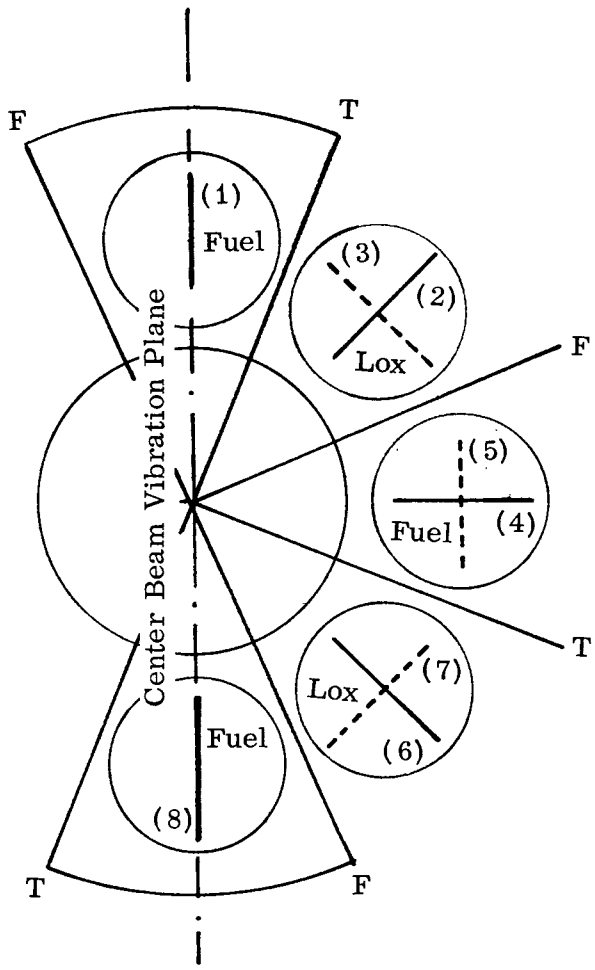

Center Beam

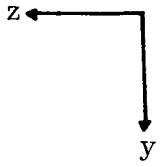

b)

Radial Vibration Planes

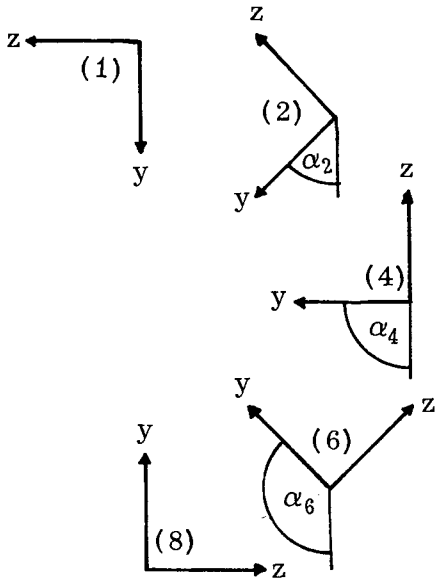

Tangential Vibration Planes

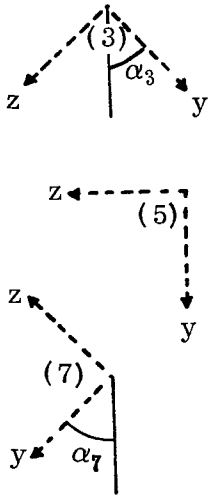

FIGURE 4. COORDINATE SYSTEMS

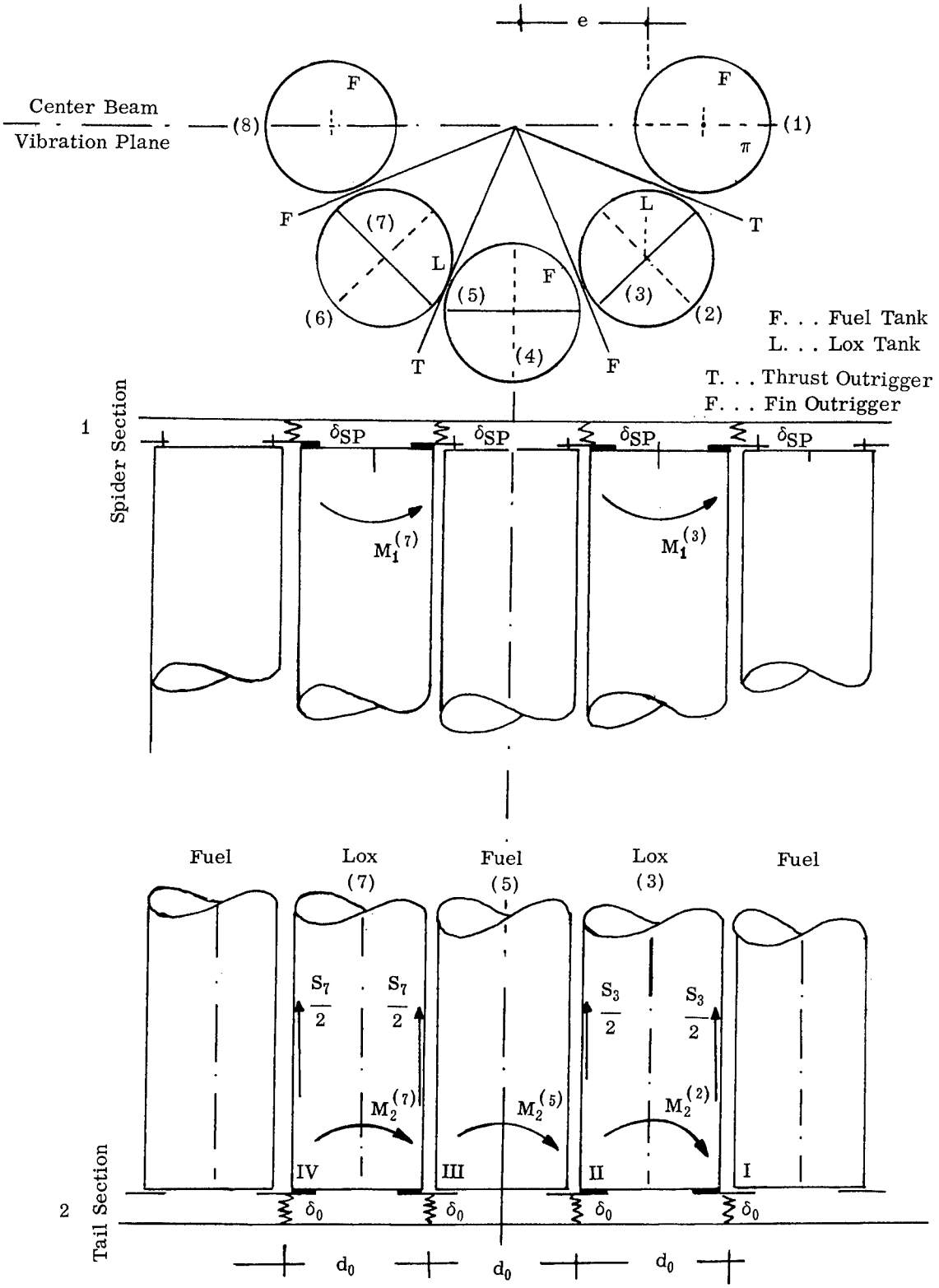

FIGURE 5. OUTER TANK SUPPORT CONDITIONS (TANGENTIAL VIBRATIONS)

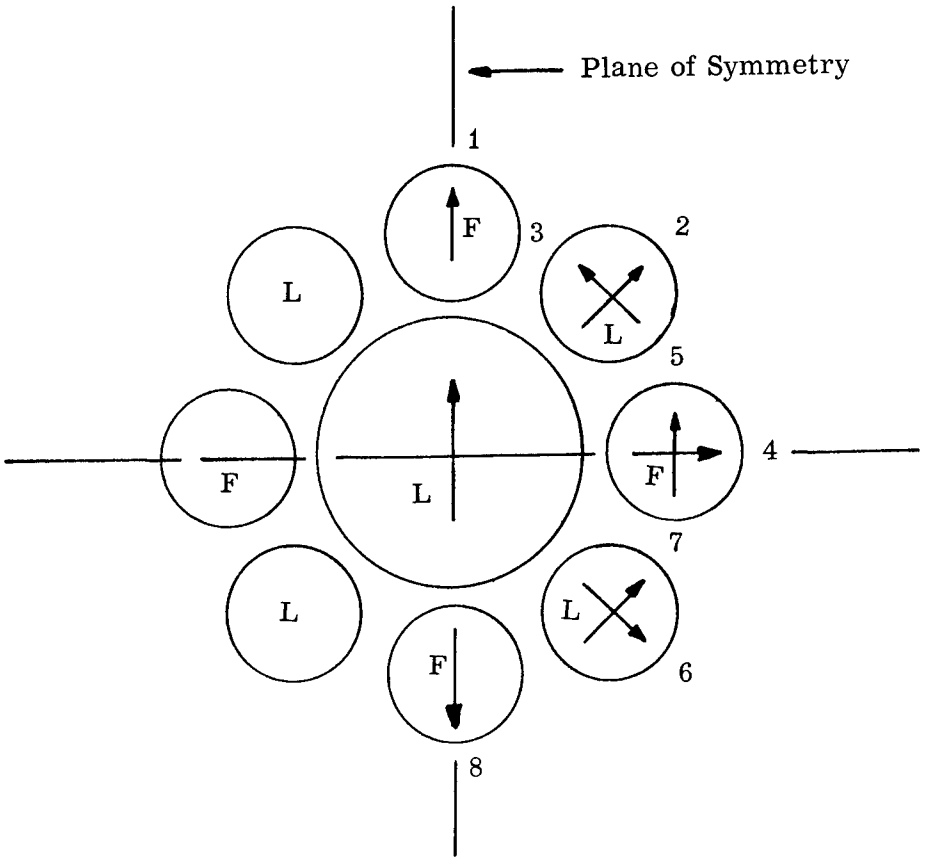

FIGURE 6. SIGN CONVENTION FOR THE VEHICLE MODE SHAPE PLOTS

The sign convention for the vehicle mode shape is positive as indicated by the arrows in the Figure above. The deflection curves of the tanks are plotted considering the following:

1. The deflection curves are plotted in the planes as indicated above and are represented in the vehicle plane of symmetry.

2. The reference axis for all deflections is the undisturbed main vehicle axis.

3. The eight planes are plotted with symmetry considered. Planes 1, 2, 3, 5, and 7 are plotted with their sign convention. Planes 6 and 8 have the same deflections as planes 2 and 1, respectively, with opposite signs. Plane 4 has no deflection.

Notice: This sign convention is opposite to that used in the analysis.

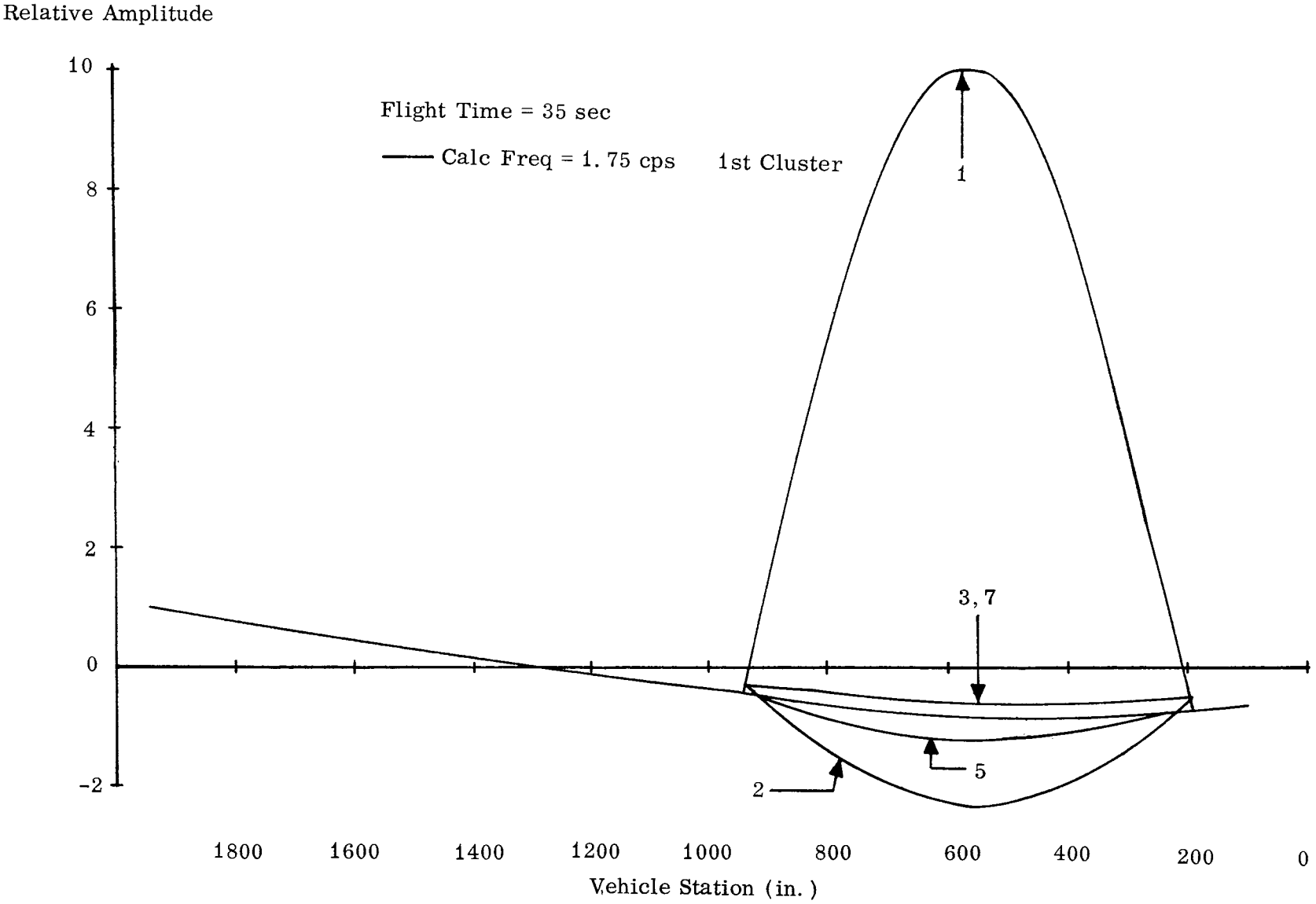

FIGURE 7. SATURN I (SAD-5) VEHICLE, RELATIVE AMPLITUDE VERSUS VEHICLE STATION

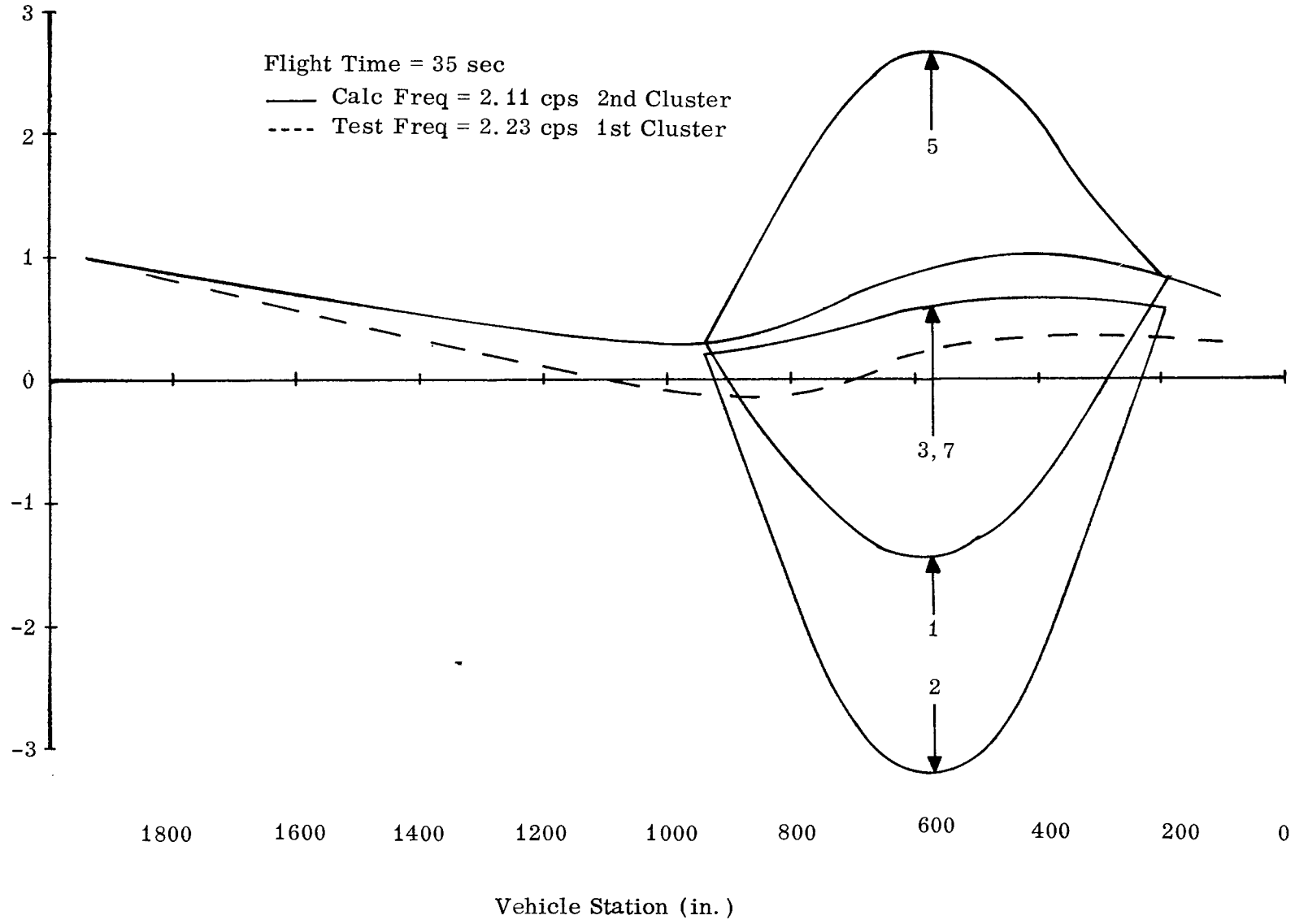

FIGURE 8. SATURN I (SAD-5) VEHICLE, RELATIVE AMPLITUDE VERSUS VEHICLE STATION

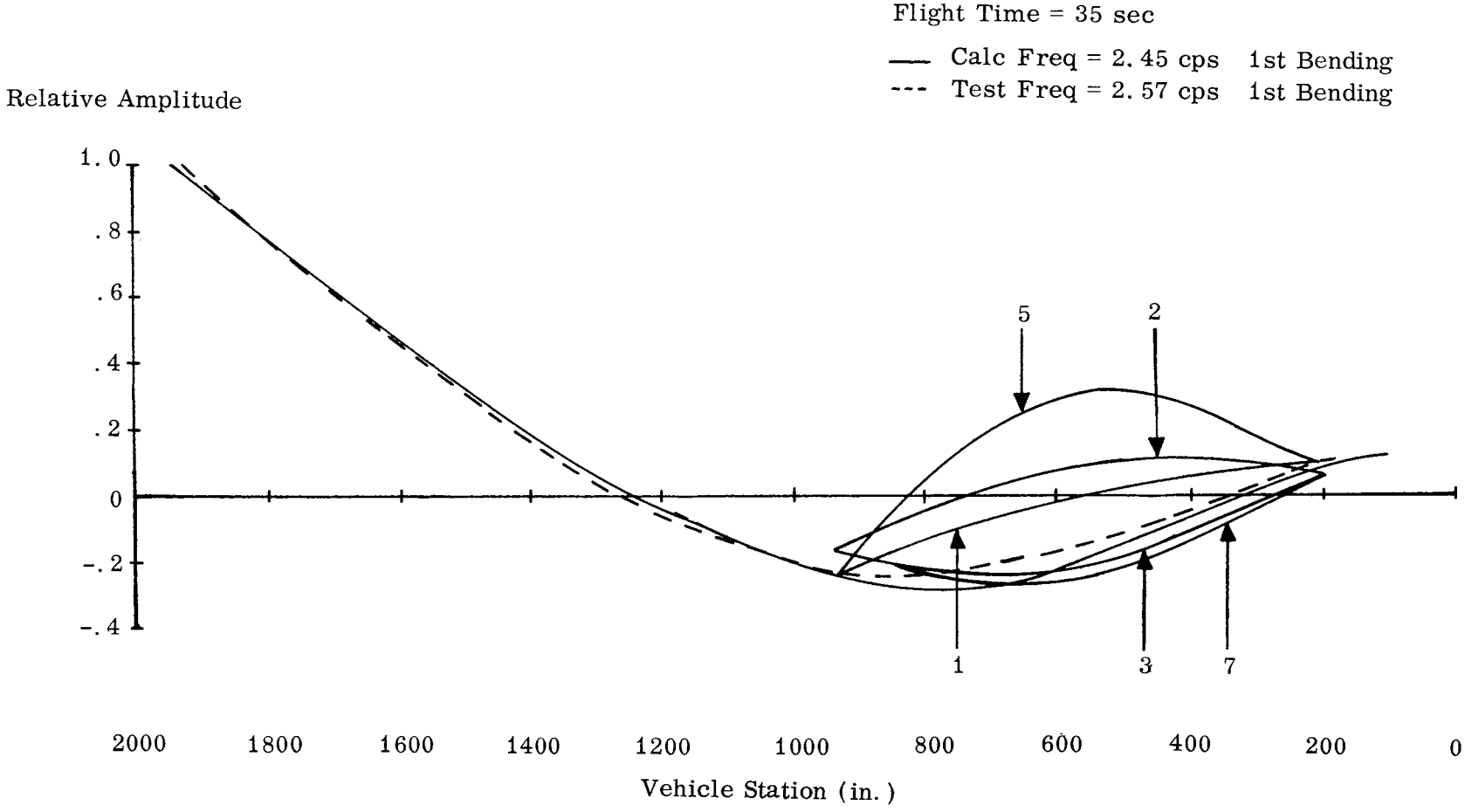

FIGURE 9. SATURN I (SAD-5) VEHICLE, RELATIVE AMPLITUDE VERSUS VEHICLE STATION

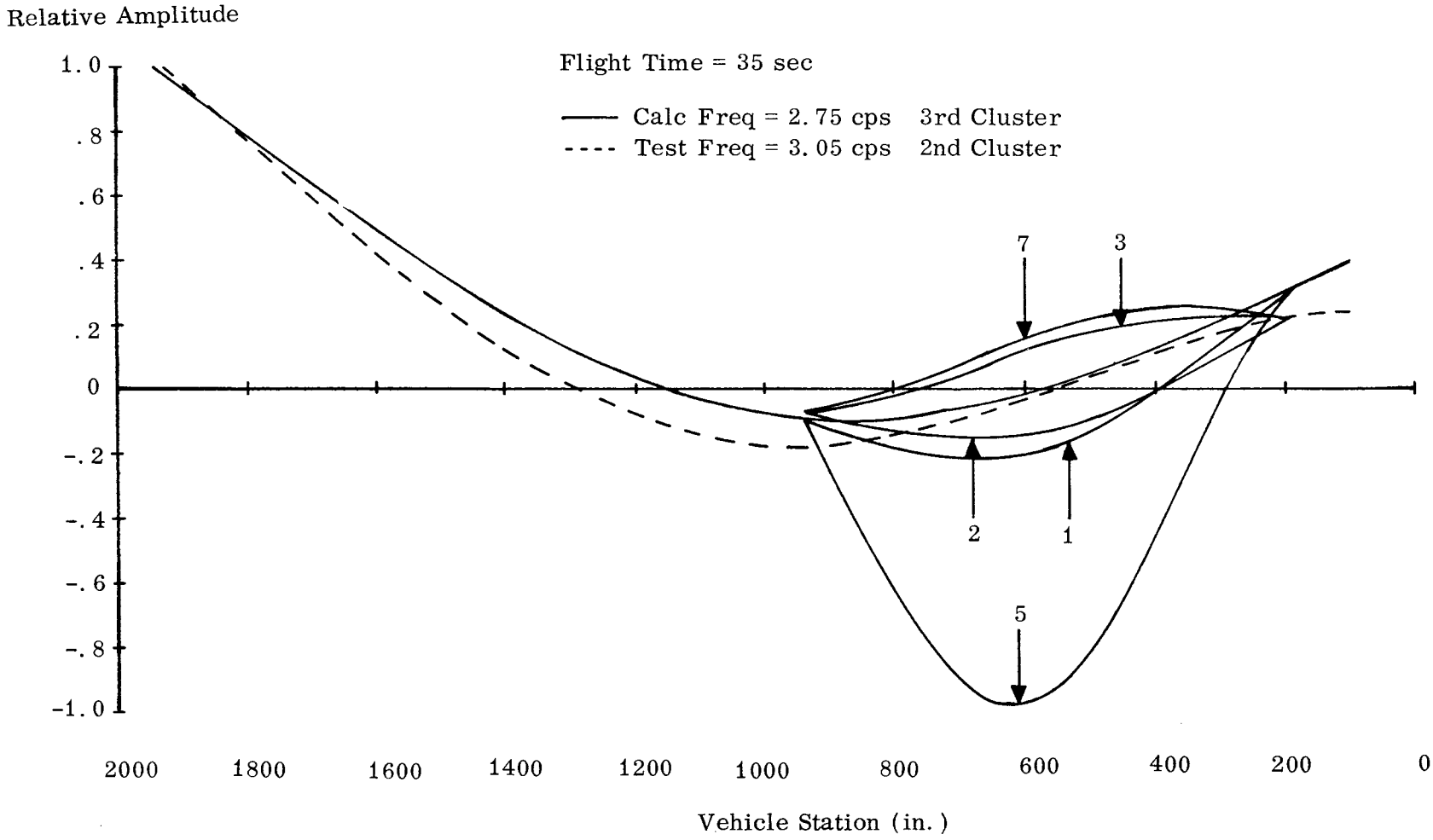

FIGURE 10. SATURN I (SAD-5) VEHICLE, RELATIVE AMPLITUDE VERSUS VEHICLE STATION

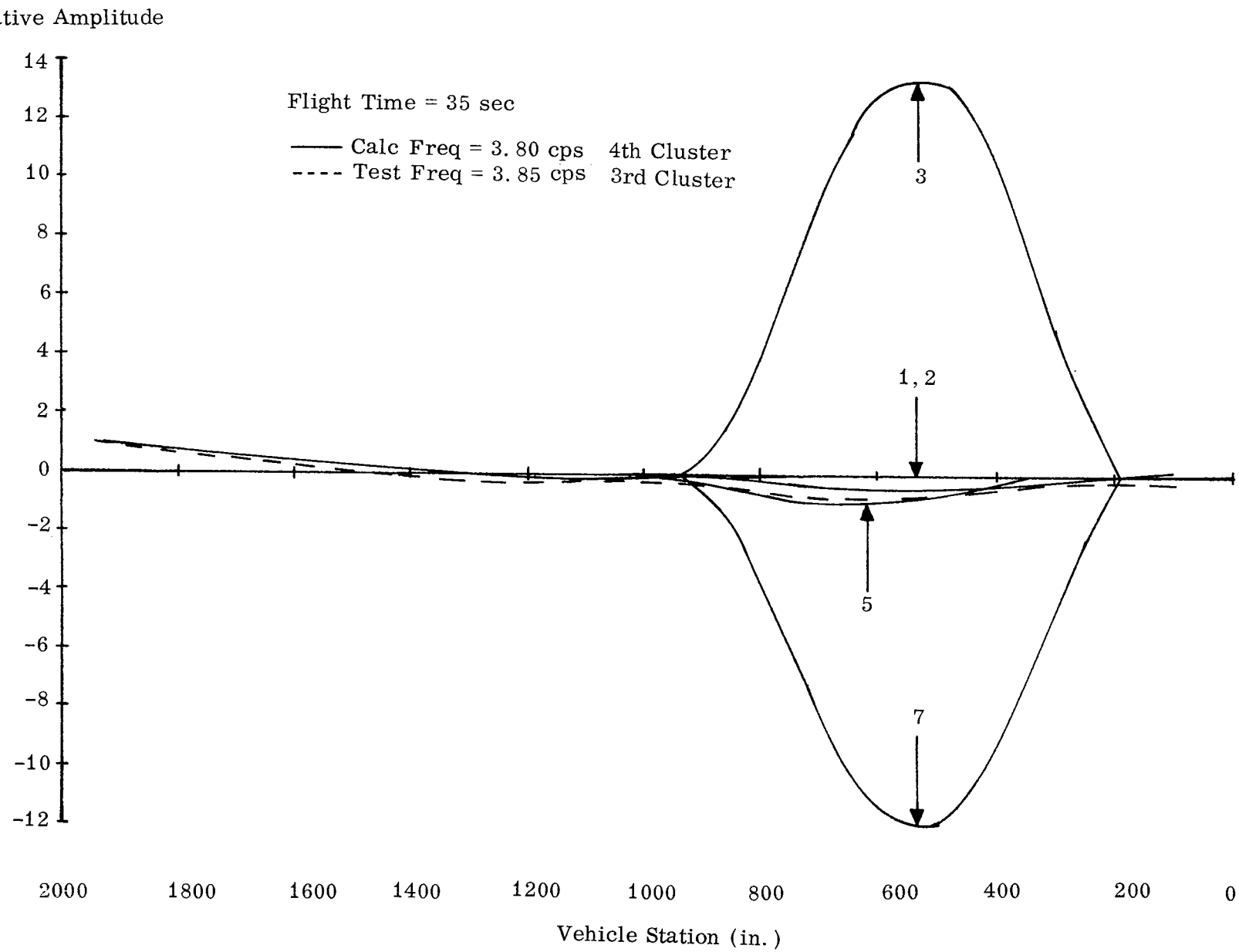

FIGURE 11. SATURN I (SAD-5) VEHICLE, RELATIVE AMPLITUDE VERSUS VEHICLE STATION

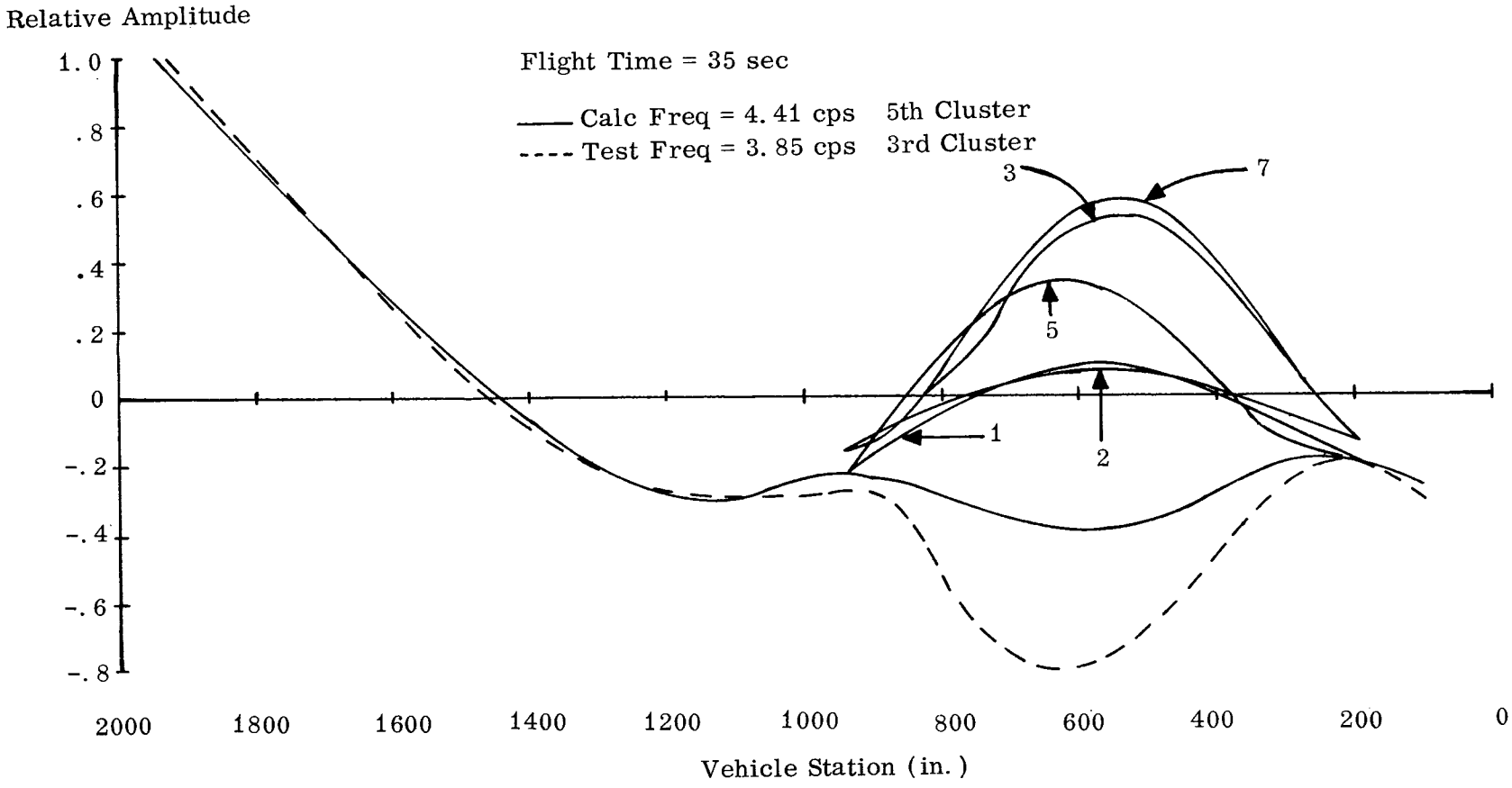

FIGURE 12. SATURN I (SAD-5) VEHICLE, RELATIVE AMPLITUDE VERSUS VEHICLE STATION

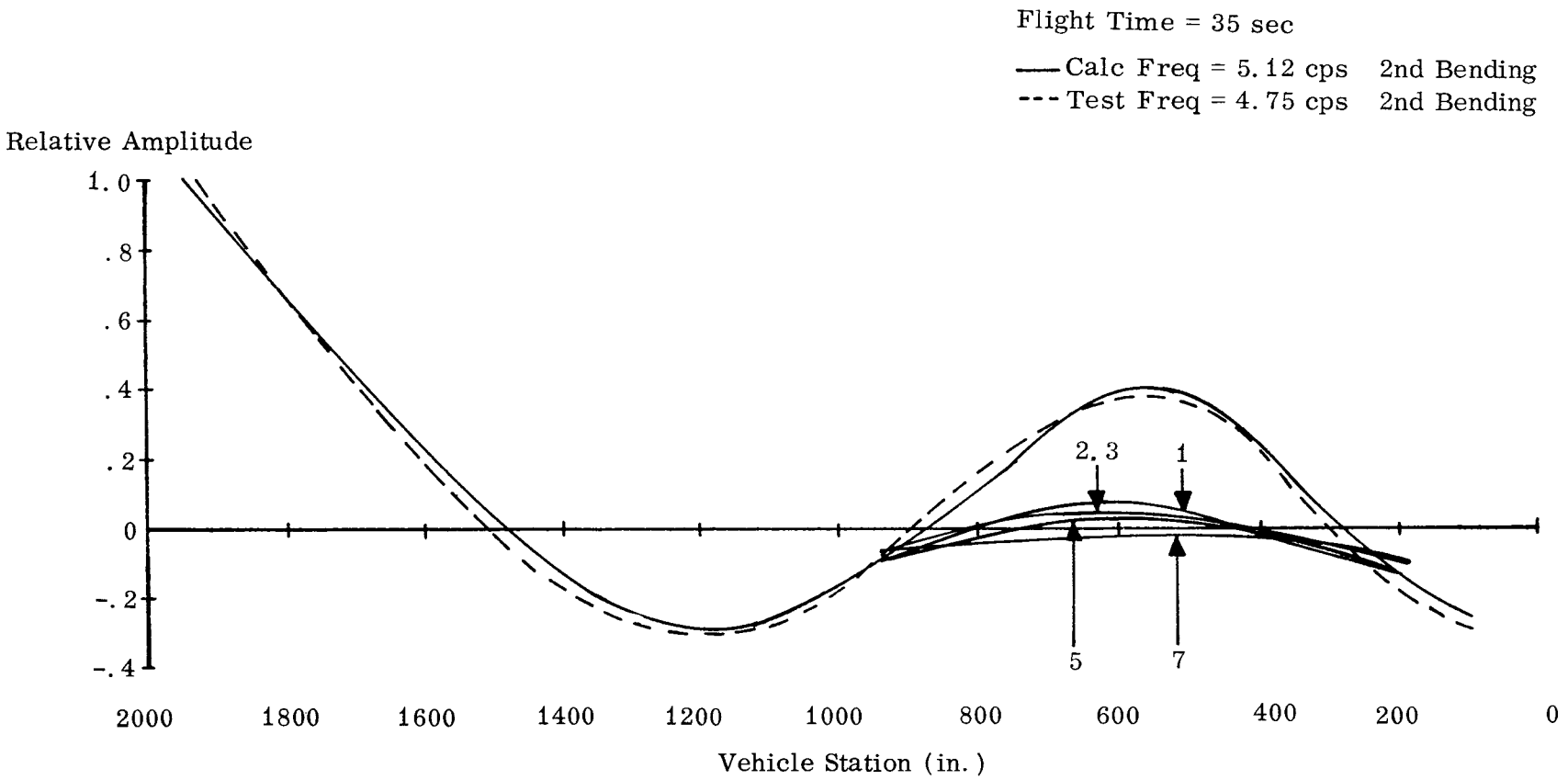

FIGURE 13. SATURN I (SAD-5) VEHICLE, RELATIVE AMPLITUDE VERSUS VEHICLE STATION

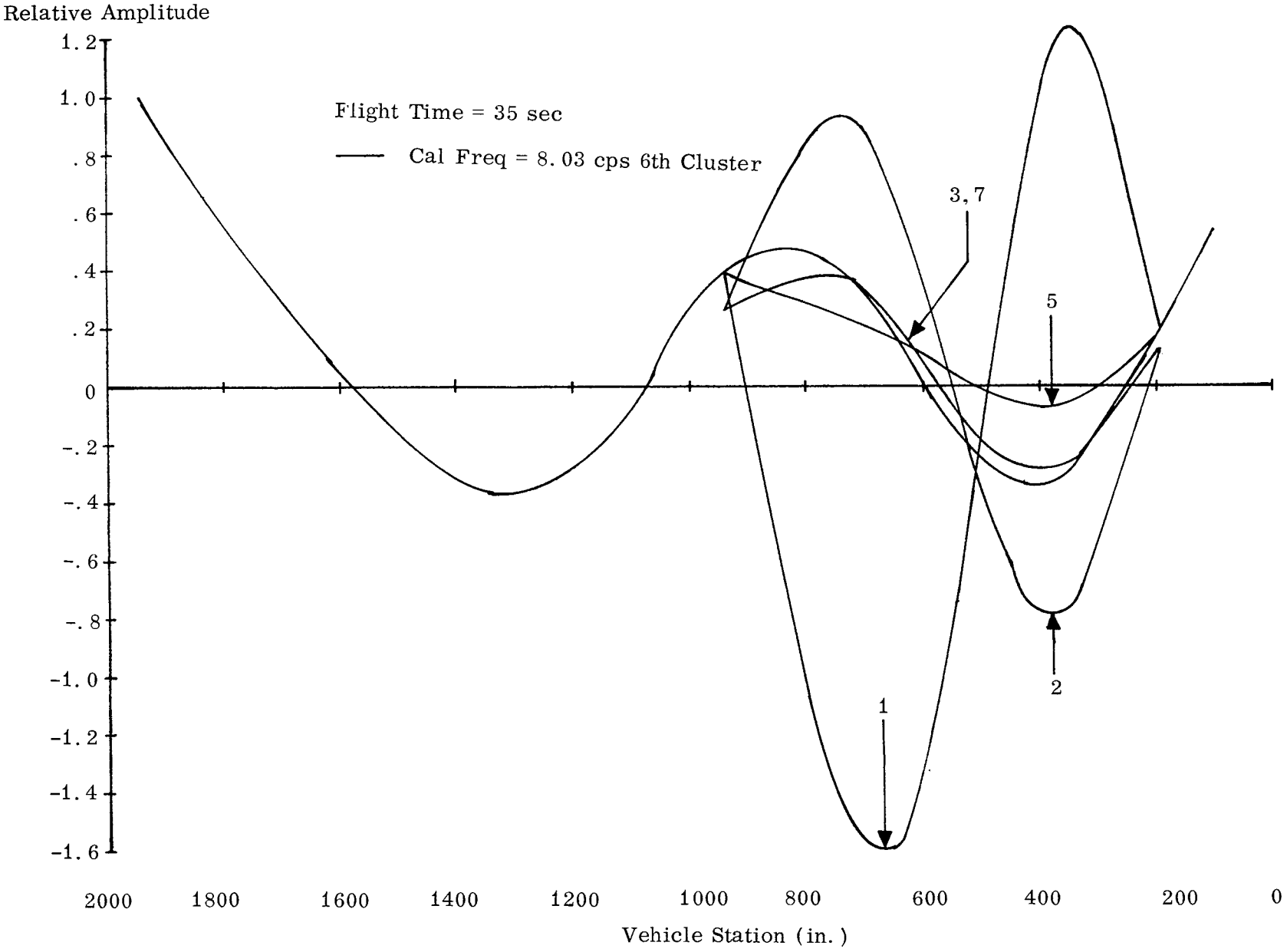

FIGURE 14. SATURN I (SAD-5) VEHICLE, RELATIVE AMPLITUDE VERSUS VEHICLE STATION

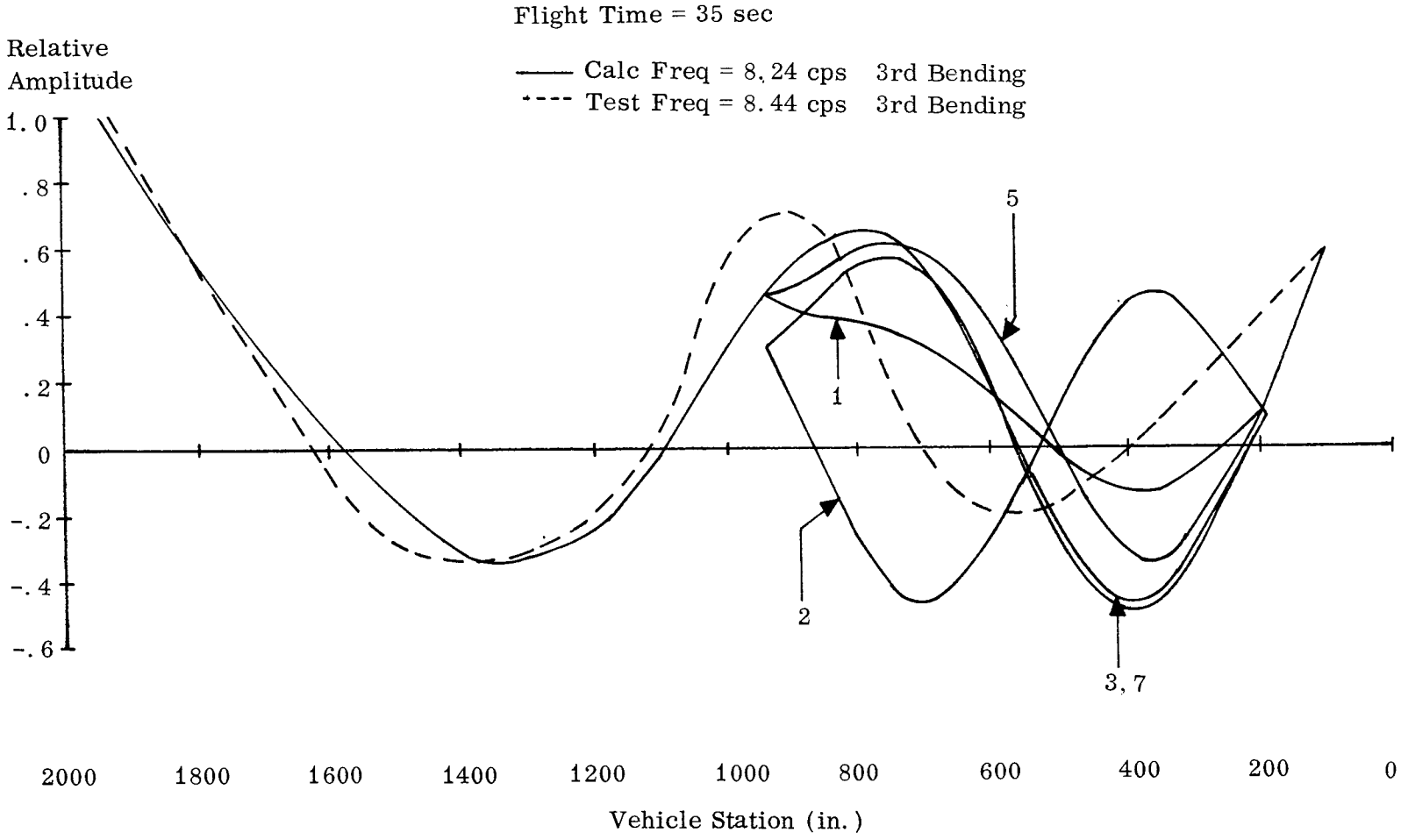

FIGURE 15. SATURN I (SAD-5) VEHICLE, RELATIVE AMPLITUDE VERSUS VEHICLE STATION

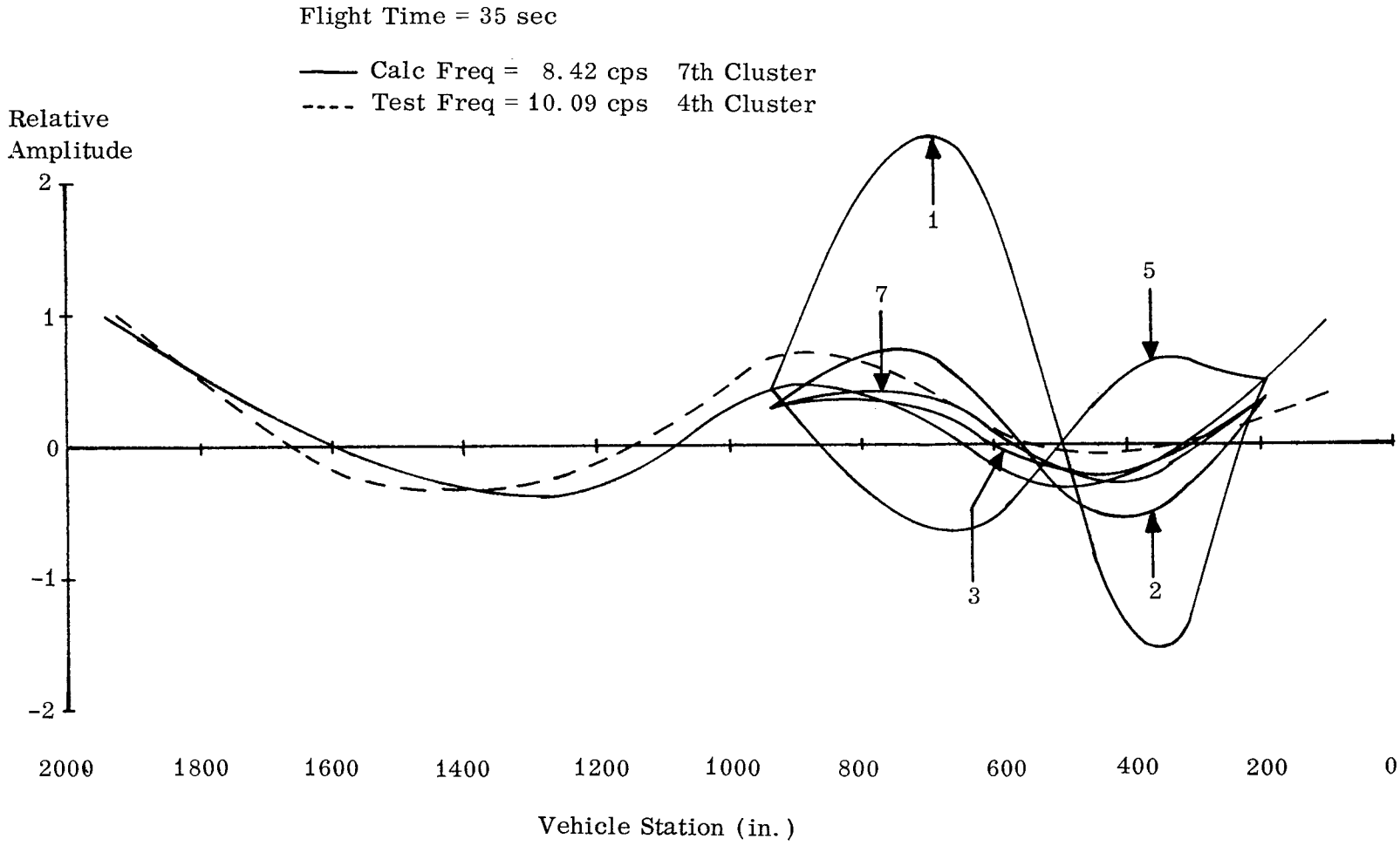

FIGURE 16. SATURN I (SAD-5) VEHICLE, RELATIVE AMPLITUDE VERSUS VEHICLE STATION

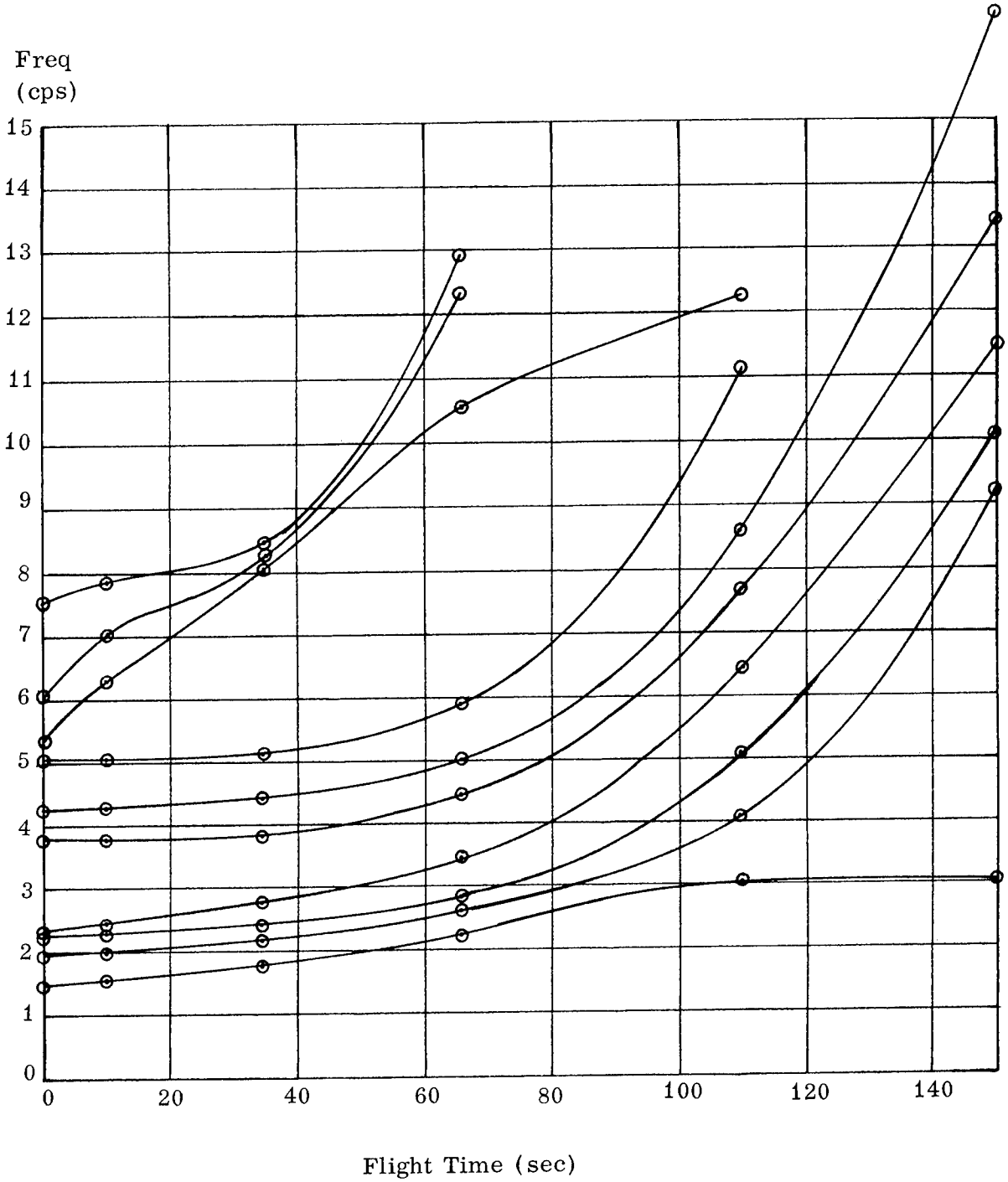

FIGURE 17. SATURN I (SAD-5) CALCULATED FREQUENCY TREND, LOWEST NATURAL FREQUENCY VERSUS FLIGHT TIME

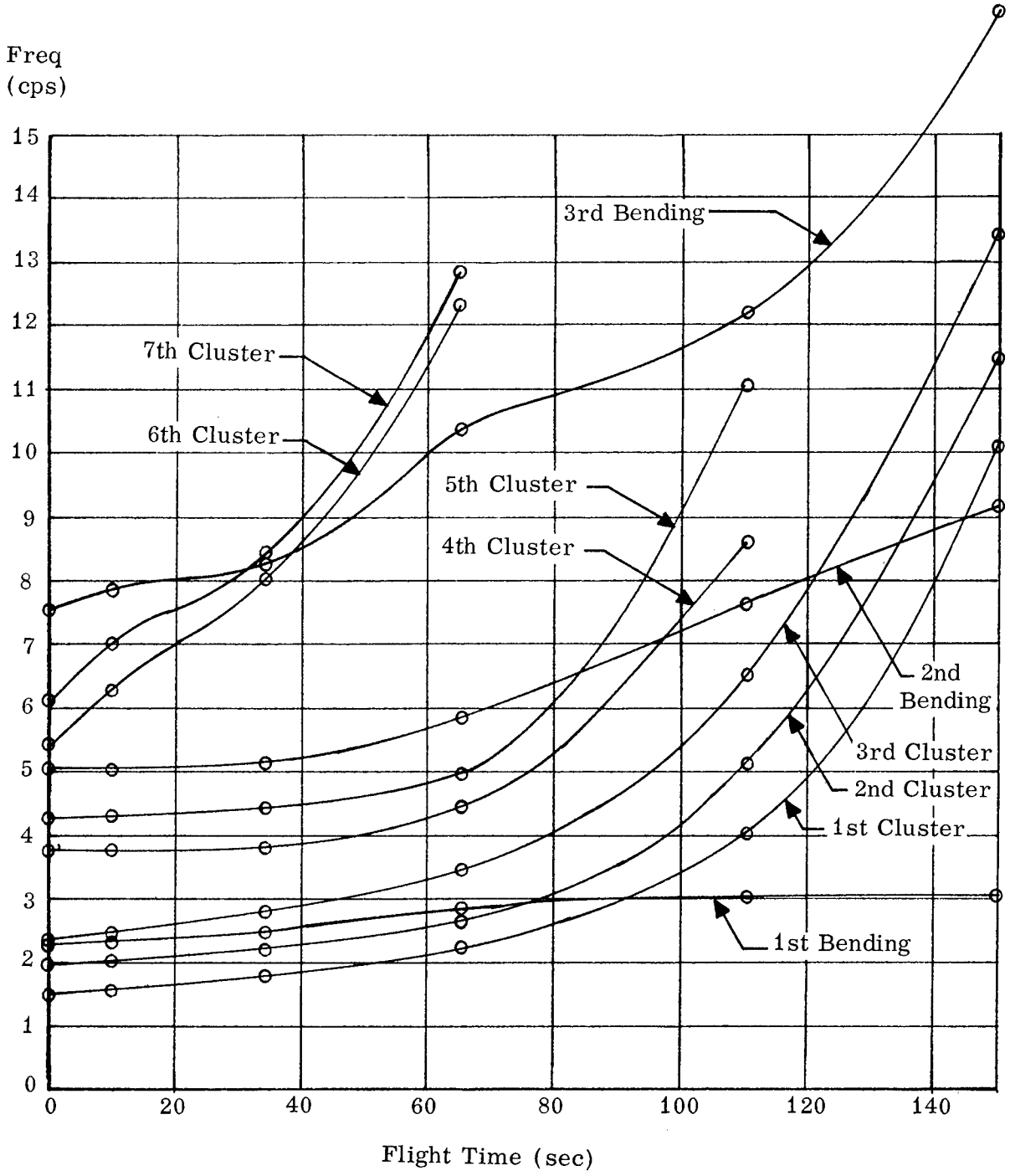

FIGURE 18. SATURN I (SAD-5) CALCULATED FREQUENCY TREND, MODE SHAPE IDENTIFICATION VERSUS FLIGHT TIME

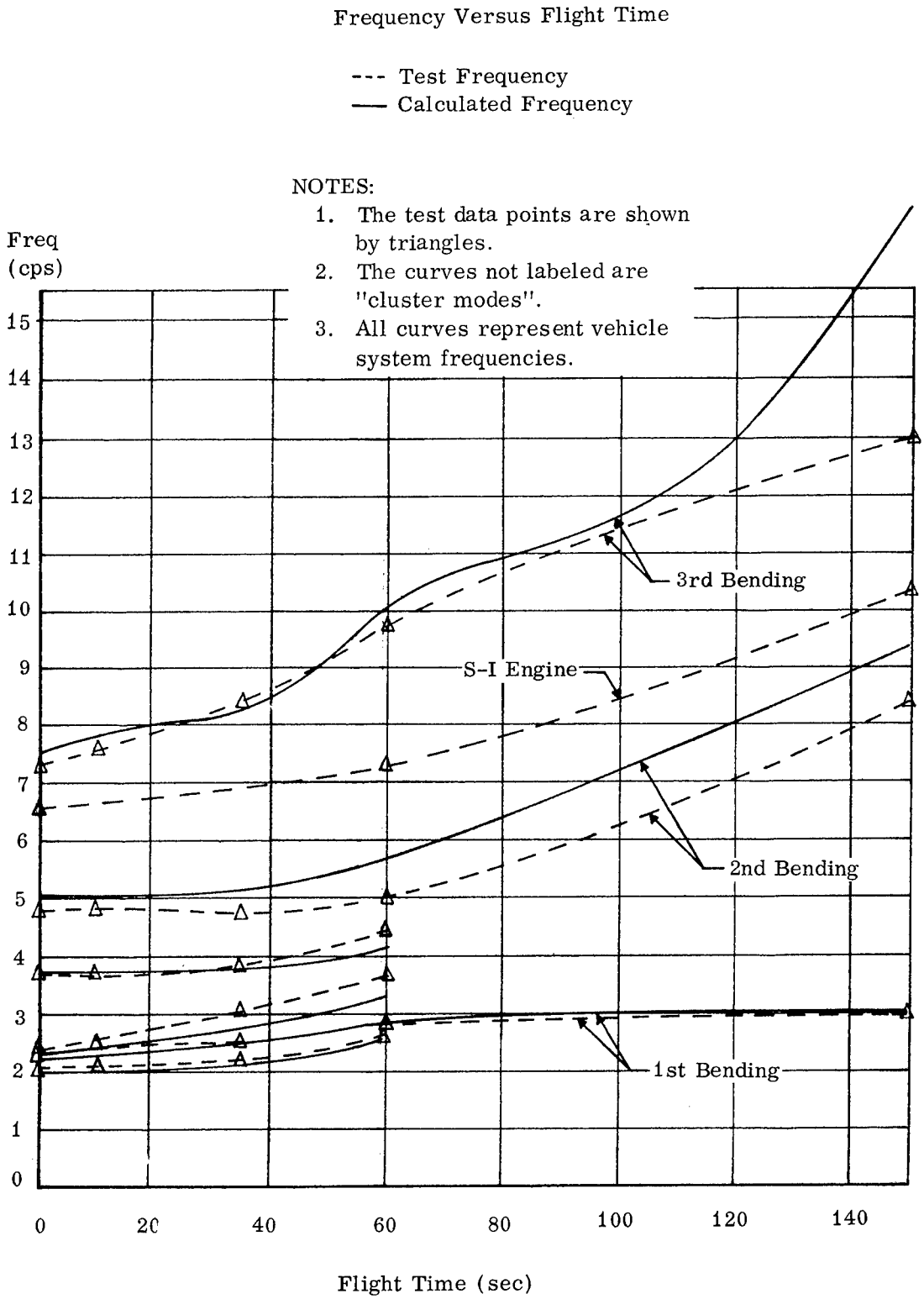

FIGURE 19. SATURN I (SAD-5) FREQUENCY COMPARISON OF REPRESENTATIVE MODE SHAPES

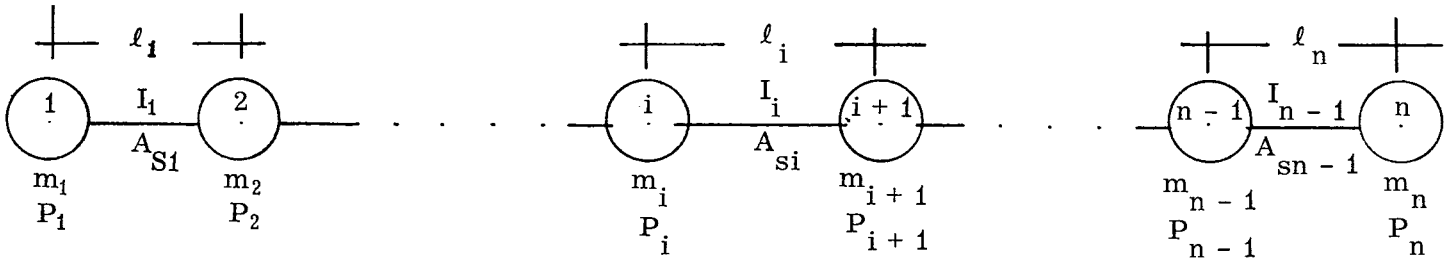

FIGURE 20a. LUMPED MASS SYSTEM

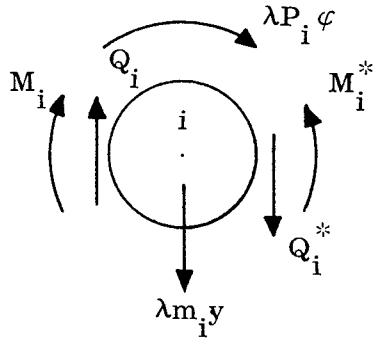

FIGURE 20b. EXTERNAL AND INTERNAL FORCES ACTING ON THE i^{th} MASS

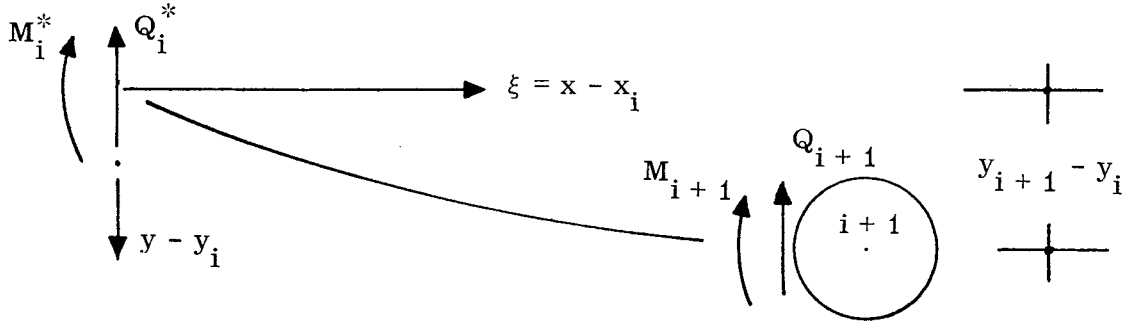

FIGURE 20c. INTERNAL FORCES ACTING ON THE i^{th} SECTION

Table 1. $\cos \alpha_i$ $i = 1, 2, \ldots 8$

Vib. plane	α_i	$\cos \alpha_i$
1	0	1
2	45°	$\sqrt{2}/2$
3	45°	$\sqrt{2}/2$
4	90°	0
5	0	1
6	135°	$-\sqrt{2}/2$
7	45°	$\sqrt{2}/2$
8	180°	-1

Table 2. Single Beam Transfers

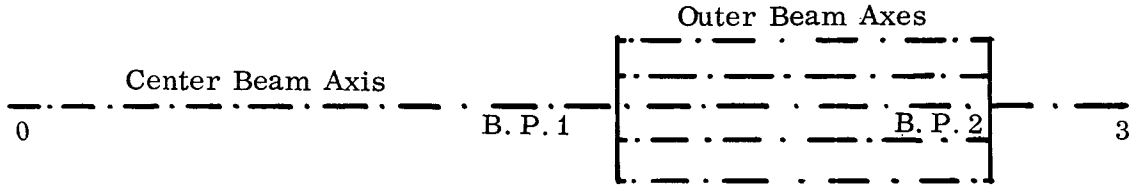

		Top 0		Branching Point 1		Branching Point 2		End 3
Center Beam	State Vectors	$y_0 = \begin{bmatrix} y_0 \\ \varphi_0 \\ M_0 \\ Q_0 \end{bmatrix}$		$y_1 = \begin{bmatrix} y_1 \\ \varphi_1 \\ M_1 \\ Q_1 \end{bmatrix}$		$y_2 = \begin{bmatrix} y_2 \\ \varphi_2 \\ M_2 \\ Q_2 \end{bmatrix}$		$y_3 = \begin{bmatrix} y_3 \\ \varphi_3 \\ M_3 \\ Q_3 \end{bmatrix}$
	Transfer Matrices		L_1		L_2		L_3	
	Transfer			$y_1 = L_1\, y_0$		$y_2 = L_2\, y_1$		$y_3 = L_3\, y_2$
Outer Beams	State Vectors			$y_1^{(i)} = \begin{bmatrix} y_1^{(i)} \\ \varphi_1^{(i)} \\ M_1^{(i)} \\ Q_1^{(i)} \end{bmatrix}$	i = 1, 4, 5, 8 Fuel i = 2, 3, 6, 7 Lox	$y_2^{(i)} = \begin{bmatrix} y_2^{(i)} \\ \varphi_2^{(i)} \\ M_2^{(i)} \\ Q_2^{(i)} \end{bmatrix}$		
	Transfer Matrices				$L_2^{(F)}$ $L_2^{(L)}$			
	Transfer					$y_2^{(i)} = L_2^{(i)}\ y_1^{(i)}$		

Table 3. Transfer of the Center Beam

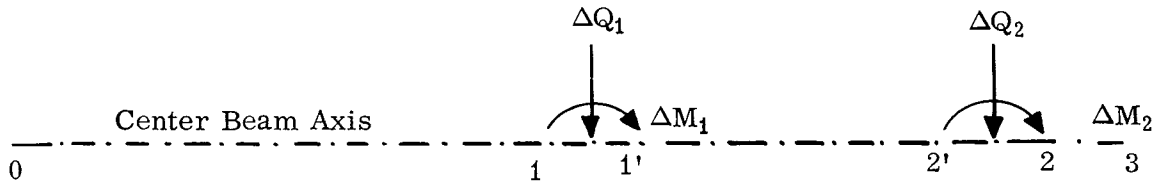

Total Launch Vehicle Model		Top 0		1		1'		2'		2		End 3
	State Vectors	$y_0 = \begin{bmatrix} y_0 \\ \varphi_0 \\ M_0 \\ Q_0 \end{bmatrix}$		$y_1 = \begin{bmatrix} y_1 \\ \varphi_1 \\ M_1 \\ Q_1 \end{bmatrix}$		$y_1' = \begin{bmatrix} y_1 \\ \varphi_1 \\ M_1' \\ Q_1' \end{bmatrix}$		$y_2' = \begin{bmatrix} y_2 \\ \varphi_2 \\ M_2' \\ Q_2' \end{bmatrix}$		$y_2 = \begin{bmatrix} y_2 \\ \varphi_2 \\ M_2 \\ Q_2 \end{bmatrix}$		$y_3 = \begin{bmatrix} y_3 \\ \varphi_3 \\ M_3 \\ Q_3 \end{bmatrix}$
	Transfer Matrices		L_1		L_1'		L_2		L_2'		L_3	
	Transfer			$y_1 = L_1 y_0$		$y_1' = L_1' y_1$		$y_2' = L_2 y_1'$		$y_2 = L_2' y_2'$		$y_3 = L_3 y_2$

Table 4. Used Matrices and Their Dimensions

Dimension	Matrices
four x four	L_i, i = 1, 2, 3; L_1^*, L_2', L_2^*, L, $L_2^{(F)}$, $L_2^{(L)}$, U_4^*, U_4, A, R, B_1, J, T_i, S_i, i = 1, 2, . . . n, L, E_1, E_n
four x eight	V_4, V_3, B_2, B_3, G, H
eight x four	V_2^*, F, Q, V_1^*, D_i, i = 1, 2, 3, 4, C_L, R_i, i = 1, 2
eight x eight	K, L_{ij}, i, j = 1, 2, 3, 4, E_i, i = 1, 2, 3, 4, U_8^*, C_M, N_{ij}, i, j = 1, 2, I

APPENDIX

TRANSFER MATRIX METHOD APPLIED TO A LUMPED MASS BEAM

A spring-supported lumped mass beam is shown by Figure 20a. It consists of masses m_i and mass moments of inertia P_i concentrated at Stations i on the beam axis (i = 1, 2, 3, ... n). The stiffness between successive stations is constant.

If it is assumed that this system is free-vibrating, following a sinusoidal law, shear and moment will obey this law also. The equilibrium conditions of the i^{th} mass (Fig. 20b) written in the amplitudes of the mentioned quantities are

$$\left.\begin{aligned} M_i^* &= \lambda P_i \varphi_i + M_i \\ Q_i^* &= -\lambda m_i y_i \end{aligned}\right\} \qquad \text{(A1)}$$

where y_i, φ_i are deflection and rotation angle at station i, M_i, Q_i. M_i^*, Q_i^* represent moment and shear at left and right side, respectively, of the i^{th} mass point. λ is the unknown parameter, of the problem,

$$\lambda = \omega^2 = 4\,\pi^2\,f^2 \qquad \text{(A2)}$$

where ω is the circular frequency and f is the natural frequency of the vibrating system.

The state in a point of the lumped mass system is determined by the state vector.

$$y = \begin{bmatrix} y \\ \varphi \\ M \\ Q \end{bmatrix}$$

From equation A1 it follows

$$\begin{bmatrix} y_i^* \\ \varphi_i^* \\ M_i^* \\ Q_i^* \end{bmatrix} = \begin{bmatrix} 1 & 0 & 0 & 0 \\ 0 & 1 & 0 & 0 \\ 0 & \lambda P_i & 1 & 0 \\ -\lambda m_i & 0 & 0 & 1 \end{bmatrix} \begin{bmatrix} y_i \\ \varphi_i \\ M_i \\ Q_i \end{bmatrix} \tag{A3}$$

$$\text{or} \qquad y_i^* = T_i\, y_i \tag{A4}$$

where the "inertia" matrix T_i is defined by equation (A3).

A similar relation exists between the state vectors y_i^* and y_{i+1} (Fig 20c).

$$y_{i+1} = S_i\, y_i \tag{A5}$$

where S_i is the stiffness matrix. S_i can be formed by solving the linear system of differential equations:

$$\left.\begin{aligned} G\, A_{si}\, (y' - \varphi) &= Q \\ -EI\, \varphi' &= M \end{aligned}\right\} \tag{A6}$$

with the boundary conditions

$$x = x_i\,; \qquad y = y_i\,; \qquad \varphi = \varphi_i \tag{A7}$$

where (Fig. 20c)

$$\left.\begin{aligned} M &= M_i^* + (x - x_i)\, Q_i^* \\ Q &= Q_i^* \end{aligned}\right\} \tag{A8}$$

The solution of equations A6 ($x = x_{i+1}$) is given by

$$\left.\begin{aligned} y_{i+1} &= y_i + \ell_i \varphi_i - \frac{\ell_i^2}{2EI_i} M_i^* - \left(\frac{\ell_i^3}{6EI_i} - \frac{\ell_i}{GA_{si}}\right) Q_i^* \\ \varphi_{i+1} &= \varphi_i - \frac{\ell_i}{EI_i} M_i^* - \frac{\ell_i^2}{2EI_i} Q_i^* \end{aligned}\right\} \qquad \text{(A9)}$$

where $\ell_i = x_{i+1} - x_i$

From equations A5, A7, A8, and A9 it follows

$$S_i = \begin{bmatrix} 1 & \ell_i & -\ell_i^2/2EI_i & -(\ell_i^3/6EI_i - \ell_i/GA_{si}) \\ 0 & 1 & -\ell_i/EI_i & -\ell_i^2/2EI_i \\ 0 & 0 & 1 & \ell_i \\ 0 & 0 & 0 & 1 \end{bmatrix}$$

Repeated application of equations A4 and A5 results in

$$\left.\begin{aligned} y_2 &= S_1 T_1 y_1 \\ y_3 &= S_2 T_2 y_2 = S_2 T_2 S_1 T_1 y_1 \\ &\cdots\cdots\cdots\cdots\cdots\cdots\cdots\cdots\cdots\cdots \\ y_i &= S_{i-1} T_{i-1} y_{i-1} = S_{i-1} T_{i-1} \cdots S_1 T_1 y_1 \\ &\cdots\cdots\cdots\cdots\cdots\cdots\cdots\cdots\cdots\cdots \\ y_n^* &= T_n y_n = T_n S_{n-1} T_{n-1} \cdots S_1 T_1 y_1 \end{aligned}\right\} \qquad \text{(A10)}$$

or $$y_n^* = L y_1 \qquad \text{(A11)}$$

where $L = T_n S_{n-1} T_{n-1} \cdots S_1 T_1$

The boundary conditions at Station 1 (Fig 20a) are

$$\left.\begin{array}{ll} Q_1 = k_1 y_1 & y_1 = \delta_1 Q_1 \\ \text{or} & \\ M_1 = -\kappa_1 \varphi_1 & \varphi_1 = -\sigma_1 M_1 \end{array}\right\} \qquad \text{(A12)}$$

where k, κ, and δ, σ represent spring constants and influence coefficients, respectively, of the beam support at Station 1.

Using matrix and vector notation, both types of conditions, from equation A12, can be combined as follows:

$$\begin{bmatrix} y_1 \\ \varphi_1 \\ M_1 \\ Q_1 \end{bmatrix} = \begin{bmatrix} 1 & 0 & 0 & \delta_1 \\ 0 & 1 & -\sigma_1 & 0 \\ 0 & -\kappa_1 & 1 & 0 \\ k_1 & 0 & 0 & 1 \end{bmatrix} \begin{bmatrix} y_1 \\ \varphi_1 \\ M_1 \\ Q_1 \end{bmatrix} \qquad \text{(A13)}$$

or

$$y_1 = E_1 y_1 \qquad \text{(A14)}$$

where the matrix E_1, is defined by equation A13. Only two of the four columns of S can be applied -- the remaining two must be changed to zero columns. The possible combinations of applicable columns are

$$1, 2;\ 3, 4;\ 1, 3;\ 2, 4 \qquad \text{(A15)}$$

What combinations should be used depends on the case in question. Obviously, a free end determined by

$$k_1 = \kappa_1 = 0 \qquad \text{or} \qquad \delta_1 = \sigma_1 = \infty$$

requires the combination 1, 2 while a fixed end given by

$$k_1 = \kappa_1 = \infty \qquad \text{or} \qquad \delta_1 = \sigma_1 = 0$$

the combination 3, 4 is required.

If none of the four quantities k, κ, δ, σ, is zero or infinite any of the above combinations can be selected.

The boundary conditions of the right end can be written

$$\left.\begin{aligned} Q_n^* + k_n y_n &= 0 \\ M_n^* - \kappa_n \varphi_n &= 0 \end{aligned}\right\} \quad \text{or} \quad \left.\begin{aligned} y_n + \delta_n Q_n &= 0 \\ \varphi_n - \sigma_n M_n^* &= 0 \end{aligned}\right\} \tag{A16}$$

Using vector and matrix notation equations A16 change over in

$$\begin{bmatrix} 1 & 0 & 0 & \delta_n \\ 0 & 1 & -\sigma_n & 0 \\ 0 & -\kappa_n & 1 & 0 \\ k_n & 0 & 0 & 1 \end{bmatrix} \begin{bmatrix} y_n \\ \varphi_n \\ M_n^* \\ Q_n^* \end{bmatrix} = \begin{bmatrix} 0 \\ 0 \\ 0 \\ 0 \end{bmatrix} \tag{A17}$$

or

$$E_n y_n^* = 0 \tag{A18}$$

where E_n is defined by equation A17.

Contrary to the case of E_1, two rows only of E_n can be applied while the remaining rows must be replaced by zero rows. The proper combinations are given again by A15.

From the first equation A11 and equations A14 and A18 it follows:

$$E_n L E_1 y_1 = 0 \tag{A19}$$

Since E_n contains two zero rows while E_1 contains two zero columns, equation A19 represents a linear homogeneous system of two equations. This system is solvable only if the determinant Δ equals zero. Δ is a polynominal in λ. The roots of $\Delta = 0$.

$$\lambda_1, \lambda_2, \lambda_3, \ldots$$

are the eigenvalues of the problem which can be found by a trial-and-error procedure. Insertion of λ_i into equation A19 yields the solution y_1, which represents the start vector. Now from application of equations A10 one obtains the state vectors of the stations and hence the i^{th} mode shape.

$$y^{(i)} = \begin{bmatrix} y_{i1} \\ y_{i2} \\ \cdot \\ \cdot \\ \cdot \\ y_{in} \\ \varphi_{i1} \\ \varphi_{i2} \\ \cdot \\ \cdot \\ \cdot \\ \varphi_{in} \end{bmatrix}$$

The i^{th} natural frequency may be calculated in accordance with equation A2.

In the case of a free beam, equation A19 may be written:

$$\begin{bmatrix} 0 & 0 & 0 & 0 \\ 0 & 0 & 0 & 0 \\ 0 & 0 & 1 & 0 \\ 0 & 0 & 0 & 1 \end{bmatrix} \begin{bmatrix} \ell_{11} & \ell_{12} & \ell_{13} & \ell_{14} \\ \ell_{21} & \ell_{22} & \ell_{23} & \ell_{24} \\ \ell_{31} & \ell_{32} & \ell_{33} & \ell_{34} \\ \ell_{41} & \ell_{42} & \ell_{43} & \ell_{44} \end{bmatrix} \begin{bmatrix} 1 & 0 & 0 & 0 \\ 0 & 1 & 0 & 0 \\ 0 & 0 & 0 & 0 \\ 0 & 0 & 0 & 0 \end{bmatrix} \begin{bmatrix} y_1 \\ \varphi_1 \\ M_1 \\ Q_1 \end{bmatrix} = \begin{bmatrix} 0 \\ 0 \\ 0 \\ 0 \end{bmatrix}$$

or

$$\left.\begin{aligned} \ell_{31}\, y_1 + \ell_{32}\, \varphi_1 &= 0 \\ \ell_{41}\, y_1 + \ell_{42}\, \varphi_2 &= 0 \end{aligned}\right\} \qquad \text{(A20)}$$

The frequency equation then follows as:

$$\begin{vmatrix} \ell_{31} & \ell_{32} \\ \ell_{41} & \ell_{42} \end{vmatrix} = 0 \qquad \text{(A21)}$$

Now λ must be determined so that equation A21 is satisfied. With this λ, equation A20, is solvable and yields the start vector.

$$y_1 = \begin{bmatrix} y_{i1} \\ \varphi_{i1} \\ 0 \\ 0 \end{bmatrix}$$

The procedure to find mode shapes and frequencies is already outlined above.

REFERENCES

1. Bullock, T., "Predicted Bending and Torsional Vibration of Saturn SA-D in Dynamic Test Tower," IN-M-S&M-S-61-13, MSFC, Huntsville, Alabama.

2. Lianis, G. and L. L. Fontenot, "Analysis of Vibrations of Clustered Boosters," ARS paper 2422-62.

3. Storey, R. E., "Dynamic Analysis of Clustered Boosters with Application to Titan III," AIAA Summer Meeting, Paper No. 63-208, June 1963.

4. Loewy, R. G., "A Matrix-Holzer Analysis for Bending Vibrations of Clustered Launch Vehicles." To be presented at the AIAA Structural Dynamics Symposium in Boston, October 1965. [1]

5. Pestel, Eduard C. and Frederick A. Leckie, "Matrix Methods in Elastomechanics," McGraw-Hill, 1963.

1. While this report was in process, the authors were informed of Loewy's paper, which appears to represent a similar approach. To show the independence of this paper, the authors point out that their Analysis has been in use at the MSFC for two years and was originally submitted to the above mentioned symposium.

"The aeronautical and space activities of the United States shall be conducted so as to contribute . . . to the expansion of human knowledge of phenomena in the atmosphere and space. The Administration shall provide for the widest practicable and appropriate dissemination of information concerning its activities and the results thereof."

—NATIONAL AERONAUTICS AND SPACE ACT OF 1958

NASA SCIENTIFIC AND TECHNICAL PUBLICATIONS

TECHNICAL REPORTS: Scientific and technical information considered important, complete, and a lasting contribution to existing knowledge.

TECHNICAL NOTES: Information less broad in scope but nevertheless of importance as a contribution to existing knowledge.

TECHNICAL MEMORANDUMS: Information receiving limited distribution because of preliminary data, security classification, or other reasons.

CONTRACTOR REPORTS: Technical information generated in connection with a NASA contract or grant and released under NASA auspices.

TECHNICAL TRANSLATIONS: Information published in a foreign language considered to merit NASA distribution in English.

TECHNICAL REPRINTS: Information derived from NASA activities and initially published in the form of journal articles.

SPECIAL PUBLICATIONS: Information derived from or of value to NASA activities but not necessarily reporting the results of individual NASA-programmed scientific efforts. Publications include conference proceedings, monographs, data compilations, handbooks, sourcebooks, and special bibliographies.

Details on the availability of these publications may be obtained from:

SCIENTIFIC AND TECHNICAL INFORMATION DIVISION

NATIONAL AERONAUTICS AND SPACE ADMINISTRATION

Washington, D.C. 20546